Computational Modelling of Water Transport in Hydrocolloid Wound Dressing, DuoDERM® CGF, and Design Recommendations

Keywords: Wound Dressings, Water Transport, Wound Healing, Hydrocolloids, Material Design

BEE 4530
Jackson Cabot, Robert Klein, Grainger Sasso, Viola Zhang
May 10th, 2018

Table of Contents

1.0 Executive Summary

Hydrocolloids, and further hydrogels, have arisen as attractive next-generation wound dressings because of their modularity and ability to retain moisture. Hydrocolloids, like DuoDERM® CGF, are intended for partial and full thickness wounds. They may be used for minor burns, cuts, tears, abrasions, as well as lacerations, ulcers, and some traumatic or surgical wounds. A computational simulation of water transport in wounds with hydrocolloid dressings was implemented in order to understand the mechanisms of hydrocolloid wound dressings as they relate to water transport. The ideal dressing will maintain the wounded tissue at physiological water content levels while also retaining moisture within the dressing itself to promote re-epithelialization of tissue. This study aims to determine the effectiveness of current wound dressings with respect to retaining moisture and maintaining the skin at physiological levels of water content. This study further seeks to optimize current wound dressing design parameters in order to improve water retention above the wound bed and maintenance of physiological skin water content.

To study the transfer of liquid water in skin and an example hydrocolloid wound dressing, a computational model was built in COMSOL Multiphysics® Modeling Software using a multifrontal direct solver (MUMPS). This model primarily detailed water transport processes in the skin (stratum corneum, epidermis, and dermis) with an example hydrocolloid dressing DuoDERM® CGF (hydrocolloid and polymeric barrier layer). The use of the model can be extended to larger or smaller wound areas as well as different types of hydrocolloid dressings. The parameters of the materials can be easily altered to fit new materials being simulated, however the model is only valid up to the time right before the hydrocolloid would start to degrade. The model considered the skin layers, wound surface, hydrocolloid, and polymeric barrier layer to be a 2D, axisymmetric cylinder. Water (mass) transport was considered diffusion in porous media in the skin and diffusion in the hydrocolloid and polymeric layers. The swelling effect, typical of hydrocolloids, was modeled using deforming geometry. After validating the model, an objective function was created in order to quantify the performance of the model based on its ability to maintain physiological water content in the skin as well as its ability to retain moisture in the hydrocolloid domain above the wound bed. Using this objective function, the material properties of the hydrocolloid dressing were altered in order to obtain an optimal solution, where the dressing would maintain an ideally moist environment.

The results confirmed that the hydrocolloid wound dressing retains moisture but does not satisfactorily maintain wounded tissue near physiological levels of water content. The optimization suggested the variation of two hydrocolloid parameters, the diffusivity and the partitioning coefficient between the skin and hydrocolloid, in order to improve its performance. Lowering the diffusivity of the hydrocolloid resulted in a higher water concentration above the wound bed. Decreasing the partition coefficient (an effect observed by increasing the hydrophobicity of the hydrocolloid) reduced the flux of water from the wound to the dressing. The combined effect of a reduced diffusivity and partition coefficient allowed greater regions of the wound to retain physiological water content levels and improved water retention near the wound bed. These results will inform the design of future generations of wound dressings and elucidate difficulties in the use of hydrophilic wound dressings like hydrocolloids and hydrogels.

Keywords: Wound Dressings, Water Transport, Wound Healing, Hydrocolloids, Material Design

2.0 Introduction

Wound healing involves many physiological parameters and metabolic processes, not all of which are well characterized. One parameter which is firmly understood to be important to the healing process is the moisture level of tissue [1]. Specifically, a moist environment has been shown to increase the rate of healing when compared to a dry scab environment [1]. Healing processes associated with a moist wound environment include: faster re-epithelialization, quicker migration of progenitor cells, and earlier appearances of growth factors [2]. Scab formation has been shown to slow the process of skin regeneration in comparison to similar wounds where scabs were prevented from forming by a moist environment [3]. Skin normally regulates the rate at which water leaves the body, preventing the catastrophic drying of underlying tissues [4]. Wounded skin loses its ability to regulate evaporative water loss; this allows for water to be lost from the underlying tissue at too rapid of a rate [1]. In a controlled study, wounded skin evaporated water at a rate as large as twenty times that of healthy skin [5]. If levels of evaporation from the wound are too great, desiccation occurs resulting in necrosis and scab formation of the wounded tissue [1],[2]. A wound which exudes too much fluid can lead to other complications such as skin maceration and increased risk of sepsis, however, the impacts of fluid accumulation in a clinical setting is highly variable and potentially benign in many cases [2]. Thus, it is important that a constant, high level of moisture be maintained for wound tissue to heal optimally; the absence of skin's moisture retaining qualities necessitates a wound dressing which can provide this functionality.

Traditional wound dressings were not designed with a controlled, optimal rate of water transport in mind. More recent developments in wound dressing technology have aimed to provide a wound environment with a moisture retentive barrier [6]. Water vapor transmission rate (WVTR) is a property that is synonymous with mass flux of water and is typically experimentally measured for both wounds and dressings[*1]. WVTR of a dressing has been shown to be a strong predictor of healing rate, although the specific physical properties of a dressing that give rise to the WVTR of a dressing are not fully understood [1],[2]. The WVTR is know to depend on the diffusivity of certain dressings which involve the diffusive transport of water [1].

There exists a very limited set of validated, quantitative measures of wound tissue surface water concentration. Measurements that do exist are for specific wound types not common to the clinical setting. The most common measure of wound moisture levels is qualitative and made visually by a physician on a point scale [2]. The ability to experimentally measure WVTR, also referred to as Transepidermal Water Loss (TEWL), quantitatively exists and has been employed for measurement of WVTR through a wound dressing in a swine model [7]. Considering the difficulties of obtaining quantitative measures of wound water concentrations, the relative availability of WVTR values of wounds and their dressings [6], and the impact the WVTR of a dressing has on the healing process, WVTR is an excellent parameter for study when investigating wound dressings and the wound healing process.

---

[1]*Note: The term WVTR does not imply that water is transported through the dressing in the gaseous form of water vapor for all dressing types. It is called this because the method that measures the mass flux of water involves the measurement of water vapor which has left the dressing surface.

The difficulties, cost, and wide variability associated with the clinical measurement of wound and wound dressing properties demand that robust, low cost avenues of analysis be pursued. COMSOL Multiphysics® Modeling Software is a fitting alternative to more analytic approaches to optimizing wound dressings. The relative ease of use and tremendous degree of control associated with numerical modeling make it an indispensable tool in the analysis of water transport within a wound, dressing, and nearby atmosphere.

2.1 Problem Statement:

There exist many difficulties and a high degree of variability when studying water concentrations and transport rates in wounds experimentally [1]. The goal of this model is to circumvent these challenges by accurately reconstructing the water transport phenomena in a wound, wound dressing, and surrounding skin with computational modeling.

2.2 Design Objectives:

The goal of this model is to elucidate the key components of water transport phenomena in wounds and wound dressings to provide informed analyses of hydrocolloid wound dressings. The objectives are to:

1. accurately model human transepidermal water loss
2. simulate wound conditions on skin transport phenomena
3. determine suitability of hydrocolloid wound dressings for wound healing
4. investigate the influence of different dressing properties and environments on skin transport phenomena
5. optimize hydrocolloid wound dressing design

With these objectives, the design and characterization of future wound dressings can be easily and rapidly improved.

3.0 Model Implementation

The model relies on the fundamental physics of water transport through human skin and biomaterials along with the observed swelling behavior of hydrocolloids. Empirical data of transport process parameters and physiological characteristics of skin were gathered from several studies for this implementation.

1. For intact skin, the dermis has a physiological water content of between 60-75% by weight [8].

This value was used to measure the success of the hydrocolloid wound dressing under the following premise: an ideal wound dressing will maintain the dermis at physiological water contents between 60% and 75% regardless of the damage to the upper layers of skin. The flux of water out of the dermis was used as a point of validation for this model.

2. At 35°C, normal skin loses water at a rate of 250 g/m^2d [5].

Studying a partial-thickness wound, the water concentration in the dermis and the flux at the wound surface is investigated in reference to the points of interest (1 and 2) defined above. Specifically, this wound is analyzed in the presence of a swelling hydrocolloid dressing and polyurethane barrier layer in order to determine if the dressing is able to maintain the wound at an optimal moisture content to promote wound healing. Further, the dressing will be evaluated for its ability to retain moisture in the domain above the wound.

3.1 Schematic:

Shown below in *Figure 1* is the schematic* of the simulated problem. The geometry of the model is two-dimensional, axisymmetric in order to model the lateral diffusion of water in partial-thickness wounds.

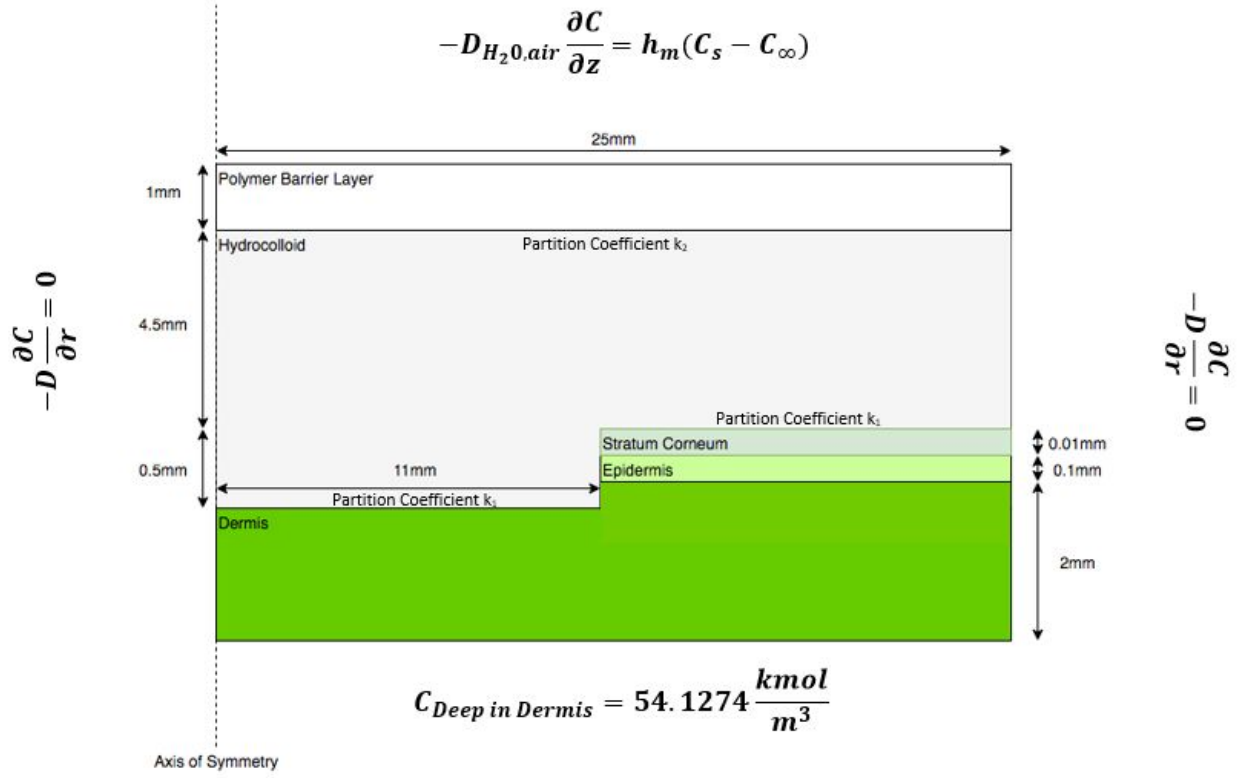

Fig. 1: **Schematic of the Problem Formulation**: The geometry, domains, dimensions, and boundary conditions are formulated above as it is computationally implemented.
*Note: Schematic not drawn to scale

The hydrocolloid being investigated, DuoDERM® CGF, contains two important components:

1. The hydrocolloid layer, used to absorb wound effuse and prevent transepidermal water loss

2. A polymeric barrier layer to prevent water diffusion into or out of the dressing from the environment.

Diffusion of moisture in air was included as a natural convective boundary condition at the boundary between the polymeric barrier layer and the environment. However, the polymeric barrier layer has a very high diffusive resistance, so the convective boundary condition is unlikely to influence the overall solution. This hypothesis was further investigated by performing a sensitivity analysis on the convective mass transfer coefficient, h_m (see *Appendix D*).

The left boundary of the model is necessarily specified as zero flux because of the conditions of axial symmetry specified by the problem formulation. The right boundary of the

model is specified with zero flux as a condition of a semi-infinite formulation: the domain was made large enough to where it can be assumed that no water diffuses at the right boundary.

The bottom boundary of the model is specified by a constant concentration. This specification was not made with a semi-infinite assumption in mind because that assumption would certainly be found invalid. Instead this specification is made in consideration of the structure of the hypodermis (the layer below the dermis), wherein blood-water perfusion is assumed to maintain the dermis at constant concentration (see *Section 3.4*).

On further note, within the schematic are the three partition coefficients: k_1, k_2, and k_3. The partition coefficients describe the ratio of concentration of water at equilibrium across the respective boundary layers, referred to as a difference in the partitioning of water. COMSOL® does not support instantiation of true partition coefficients using relations purely of concentration. Instead, these partition coefficients were implemented in flux boundary conditions between the two surfaces (see *Section 3.4*).

For more information on mathematical implementation of these boundary conditions and information on the parameters and assumptions used in the model, please see the section below: *3.4 Boundary Conditions*.

3.2 Governing Equations:

The first set of governing equations used for this model involve the various transport processes of water within the three specified domains: skin layers, hydrocolloid, and polymeric barrier layer.

Water is transported in the skin layers (dermis, epidermis, and stratum corneum) via diffusion processes in porous media, which is described in equation (1).

$$\frac{\partial c}{\partial t} = D_{AB}\left[\frac{1}{r}\frac{\partial}{\partial r}\left(r\frac{\partial c}{\partial r}\right) + \frac{\partial^2 c}{\partial z^2}\right] \qquad (1)$$

where D_{AB} is water diffusivity in the skin and c is the water concentration.

Water is transported in the hydrocolloid via diffusion and convection (due to swelling), which is described in equation (2).

$$\frac{\partial c}{\partial t} + \left[\frac{\partial (u_r c)}{\partial r} + \frac{\partial (u_z c)}{\partial z}\right] = D_{AB}\left[\frac{1}{r}\frac{\partial}{\partial r}\left(r\frac{\partial c}{\partial r}\right) + \frac{\partial^2 c}{\partial z^2}\right] \qquad (2)$$

where D_{AB} is water diffusivity, $\mathbf{u}$ is the velocity of swelling, and c is the water concentration. For more information on this condition, see section *3.3 Swelling*.

Water is transported in the polymeric barrier layer through simple diffusion as described in equation (3).

$$\frac{\partial c}{\partial t} = D_{AB}[\frac{1}{r}\frac{\partial}{\partial r}(r\frac{\partial c}{\partial r}) + \frac{\partial^2 c}{\partial z^2}] \quad (3)$$

where D_{AB} is water diffusivity in the polymeric barrier layer and and c is the water concentration.

3.3 Swelling:

Polymer swelling is characterized with an equilibrium theory developed by Flory and Rehner, in which the physicochemical properties of the material are considered [9]. However, the macroscopic level of swelling is of concern for real-life wound treatment. A dynamic polymer swelling model represents hydrocolloid dressing swelling. This model is based on a modified Fick's second law of diffusion that accounts for the convective effects of mass transport of solvent as the concentration of the diffusing species influences overall swelling. Fick's second law of diffusion models swelling in the case when the relaxation time of the polymer is much shorter than the characteristic diffusion time for solvent transport.

The change in volume of a hydrocolloid is a function of time because solvent transport is controlled by a concentration gradient dependent on time [10]. The swelling velocity (the axial displacement of the hydrocolloid/polymer boundary layer over time) of the hydrocolloid DuoDERM® CGF is empirically derived as:

$$V(t) = (3.70 - 2.206 \cdot 10^{-5} t)\, 1 \cdot 10^{-8}\ [\text{m/s}] \quad (4)$$

Swelling in the polymer barrier layer is not considered in the model because the expansion is negligible due to its material properties; thus, swelling is only implemented in the hydrocolloid [6].

The implementation of swelling in COMSOL® involved a deformed geometry because the total volume of the domain changes when mass is being added [29]. Water input into the hydrocolloid is the physical cause of the swelling. This input and swelling is represented by V(t). The hydrocolloid domain was allowed to freely deform in the z-direction. The geometry is fixed in the radial direction because the model is semi-infinite in that direction. The barrier layer does not have swelling velocity in reference to itself, thus it is carried along in distance due to the hydrocolloid.

3.4 Boundary Conditions:

The convective boundary condition at the surface of the polymeric barrier layer was modelled by:

$$-D_{AB}\frac{\partial c}{\partial z}|_{z=7.61mm} = h_m\ (c_{surface} - c_{bulk}) \tag{5}$$

where h_m is the convective mass transfer coefficient calculated using Sherwood's number for flat horizontal plate natural convection taking into account Sutherland's formula for viscosity (Refer to Appendix C).

The boundary condition at r = 0 mm is zero flux as described in equation (6) below.

$$-D_{AB}\frac{\partial c}{\partial r}|_{r=0\ mm} = 0 \tag{6}$$

This condition arises from the assumption of axial symmetry. In other words the flux across the axis of symmetry is necessarily zero by the assumption of axial symmetry.

The boundary condition at r = 25 mm is zero flux as described in equation (7) below.

$$-D_{AB}\frac{\partial c}{\partial r}|_{r=25\ mm} = 0 \tag{7}$$

This condition arises from the assumption of a semi-infinite geometry.

The boundary condition at z = 0 mm is a constant concentration as described in equation (8) below.

$$c|_{z=0\ mm} = 54.1274\frac{kmol}{m^3} \tag{8}$$

Where 54.1274 kmol m^{-3} is the initial concentration of water in the dermis. This boundary was specified as constant concentration because the hypodermis (the layer of skin below the dermis) was assumed to remain at constant water concentration.

This assumption was based on water content and blood-water perfusion equilibrium in the hypodermis. Specifically, the hypodermis consists of adipose tissue perfused with water by blood vessels. The amount of perfusion from the blood vessels is a function of the osmotic gradient between the blood and the interstitium of the adipose tissue as well as the osmotic pressure of the adipose cells themselves [11]. For the purposes of this model, this effect was simplified to the boundary condition shown above: the bottom of the dermis remains at approximately constant concentration. This assumption was made because the transport of water out of the dermis should yield higher ionic and solute concentration, thus a higher osmotic pressure, which will cause water to perfuse from the adipose tissue into the dermis. The water that perfused out of the adipose tissue will then be replaced through blood-water perfusion.

A more complete model of skin-water transport would include the perfusion of water in the skin through osmolarity and ionic transport as was investigated by van Kemanade in her 1998 thesis [12]; however, this was deemed unnecessary for the goal of this model. Specifically, it was deemed the accurate modelling of blood-water perfusion was unnecessary to optimize the characteristics of the hydrocolloid because these characteristics concern more the flux of water directly at the wound surface.

3.5 Partitioning:

In general, a partition coefficient defines the ratio of concentrations of a solute in two solids (or immiscible fluids) at equilibrium. A general mathematical description of a partition coefficient can be seen in equation (9) below.

$$c_{solid\,1} = k^* c_{solid\,2} \tag{9}$$

Where k^* is defined as the partition coefficient between solid 1 and solid 2.

Within this model, there exists three different partition coefficients k_1, k_2, and k_3 that define the partitioning between skin and hydrocolloid, hydrocolloid and polymeric barrier layer, and polymeric barrier layer and air respectively. Although the relationship defined in equation (9) above is the correct implementation of partition coefficients, COMSOL® is unable to process this type of boundary condition because it results in an essentially infinite derivative of concentration at the boundary and an ultimately divergent solution. To implement these partition coefficients in COMSOL®, a flux boundary condition was implemented as described in equations (10, 11) below:

$$-D_{AB}\frac{\partial c}{\partial r}|_{boundary\,1} = h_m(c_1 - c_2 k^*) \tag{10}$$

$$-D_{AB}\frac{\partial c}{\partial r}|_{boundary\,2} = -h_m(c_1 - c_2 k^*) \tag{11}$$

Where D_{AB} is water diffusivity, h_m is the mass transfer coefficient, and k^* is the partition coefficient.

For implementation of the partitioning in COMSOL®, the mass transfer coefficient was chosen to be arbitrarily large in order to approach equation (9) above, which is essentially the limit of equations (10, 11) as h_m approaches infinity. It is important to note, however, that h_m cannot be made too large or the possibility of a divergent solution will again be an issue. This implementation of partition coefficients effectively enforces the concentration discontinuity condition while also maintaining flux continuity throughout the domain [13].

Equations (10, 11) were used to implement a partition coefficient between the skin and the hydrocolloid as well as between the hydrocolloid and the polymeric barrier layer. The partition coefficient between the polymeric barrier layer and the air was included in the calculation of the mass transfer coefficient, h_m. For more information on this implementation, see *Section 3.4 Boundary Conditions*.

The partition coefficient between the stratum corneum and pure water is a known value [14]. This value was directly implemented as the partition coefficient between the skin and hydrocolloid because the hydrocolloid is mostly water at maximal hydration.

The partition coefficient between the hydrocolloid and the polymeric barrier layer was calculated as the ratio of the solubilities of water in the two materials. The partition coefficient between the polymeric barrier layer and air was estimated and analyzed.

3.6 Initial Conditions:

The initial conditions of the model were specified under isolated conditions. For instance, the initial water content of the skin was specified as though no wound were present. Further, the initial concentration of the hydrocolloid and polymeric barrier layer were specified as though both had been freshly removed from the package. Although these descriptions entail an assumption−and therefore a reduction in accuracy−these assumptions are not too distinct from reality. For instance, it is likely that a patient will suffer a burn and be in a hospital in less than 20 minutes before having a hydrocolloid dressing applied. The span of 20 minutes from burn to treatment and the span of 1 minute between DuoDERM ® CGF removal from its package and application likely will not greatly influence their respective water contents. Much of the data for skin water concentration is given in terms of water content (a percentage). For a list of material properties and initial conditions, see *Appendix C*.

3.7 Numerical Implementation:

The equations are solved using a commercial finite element package, COMSOL® Multiphysics version 5.3 (COMSOL Multiphysics Burlington, MA). Three modules in this software were used: *Transport of Diluted Species in Porous Media*, *Transport of Diluted Species*, and *Deformed Geometry*. *Transport of Diluted Species in Porous Media* solved for equation (1); *Transport of Diluted Species* solved for equations (2, 3); *Deformed Geometry* solved for equation (4) as it related to the velocity of the hydrocolloid boundary layer with the polymeric barrier layer. A backward time difference discretization with an initial time step of 0.001 hours and a maximum time step of 0.1 hours was used thereafter. The relative and absolute tolerances values were 0.01. A mesh of 112870 elements was used for the 2D model for which the maximum element size was set to 5.1 μm for the stratum corneum layer, 26 mm for the epidermis layer, 51 μm for the area below the wound surface, and 0.74 mm for the rest of the domain. A MUltifrontal Massively Parallel sparse direct Solver (MUMPS) was used with an automatic non-linear solver. Computation run times varied from 15 minutes to 1 hour with 16 GB of RAM on a 3.40 GHz quad core Intel^{R} i7-6700 CPU processor.

4.0 Convergence and Validation

In order for this model to be relevant to inform physicians, manufacturers, and researchers on the utility of hydrocolloid wound dressings, it is necessary to demonstrate that the model accurately depicts the transport processes. Firstly, the discretization error must be minimized by demonstrating that the solution no longer experiences large changes as a result of changes in the mesh size or time step size (known as convergence). Secondly, the values produced by the model must be compared to experimental results to ensure that the outcome of the model is physically accurate.

4.1 Mesh Construction:

An important step in the discretization of a physical phenomena with a computational model is the generation of meshing. Depicted below is the mesh that was generated to effectively discretize the model. The regions of high mesh density coincide with regions that experience the greatest concentration gradients. Such regions necessitate a high degree of spatial resolution to avoid discretization errors in the solution. A high mesh density was also used in a key region of interest: the region of dermal tissue just below the wound surface.

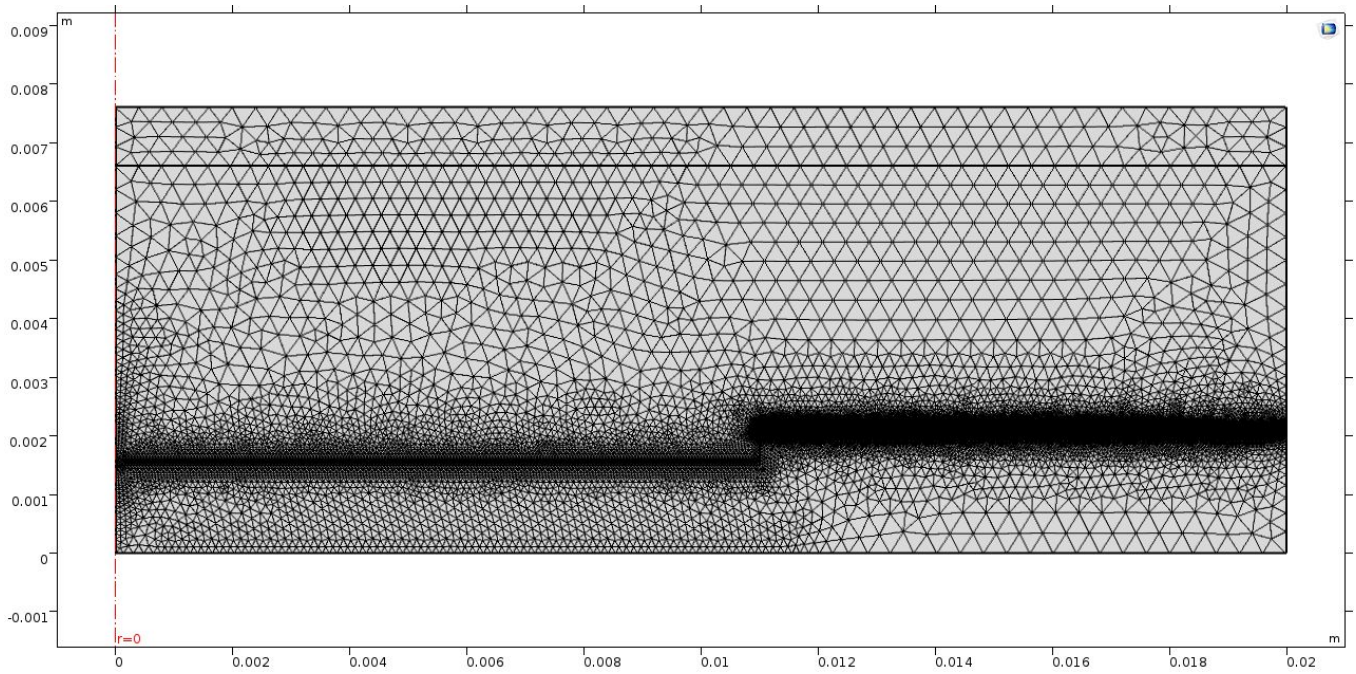

Fig. 2: **Overview of Mesh Scheme**: Note the extremely high meshing densities in the epidermis and stratum corneum layer, as well as the region below the wound surface.

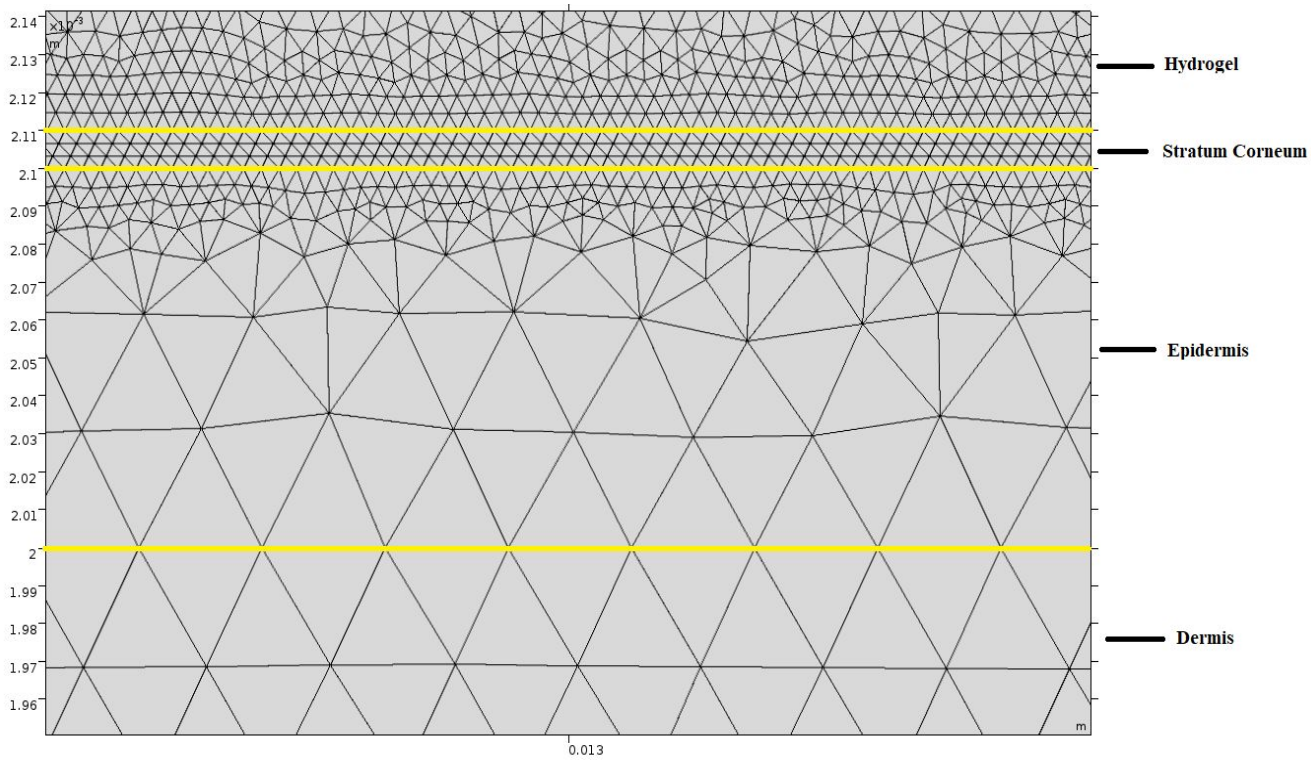

Fig. 3: **Higher Resolution Image of the Dermis, Epidermis, Stratum Corneum Layers and Hydrocolloid Meshing:** The high mesh density used here was necessary to avoid any discretization error in the stratum corneum layer.

As seen above, meshing density increases in regions where high concentration gradients are expected, such as the interface between the wound and hydrocolloid where there is a discontinuous jump in concentration due to the partition coefficient. It is crucial to mesh each domain with a sufficient number of elements, especially the stratum corneum. The stratum corneum is very thin and will not contain any nodes if there is not a sufficiently fine mesh.

4.2 Time Step Convergence:

Investigating the effect that the maximum time step has on the results of the model is another step in addressing discretization error. The solution utilizing a default maximum time step was compared with the solution from a one order of magnitude reduction in the maximum time step depicted below in *Figure 4*.

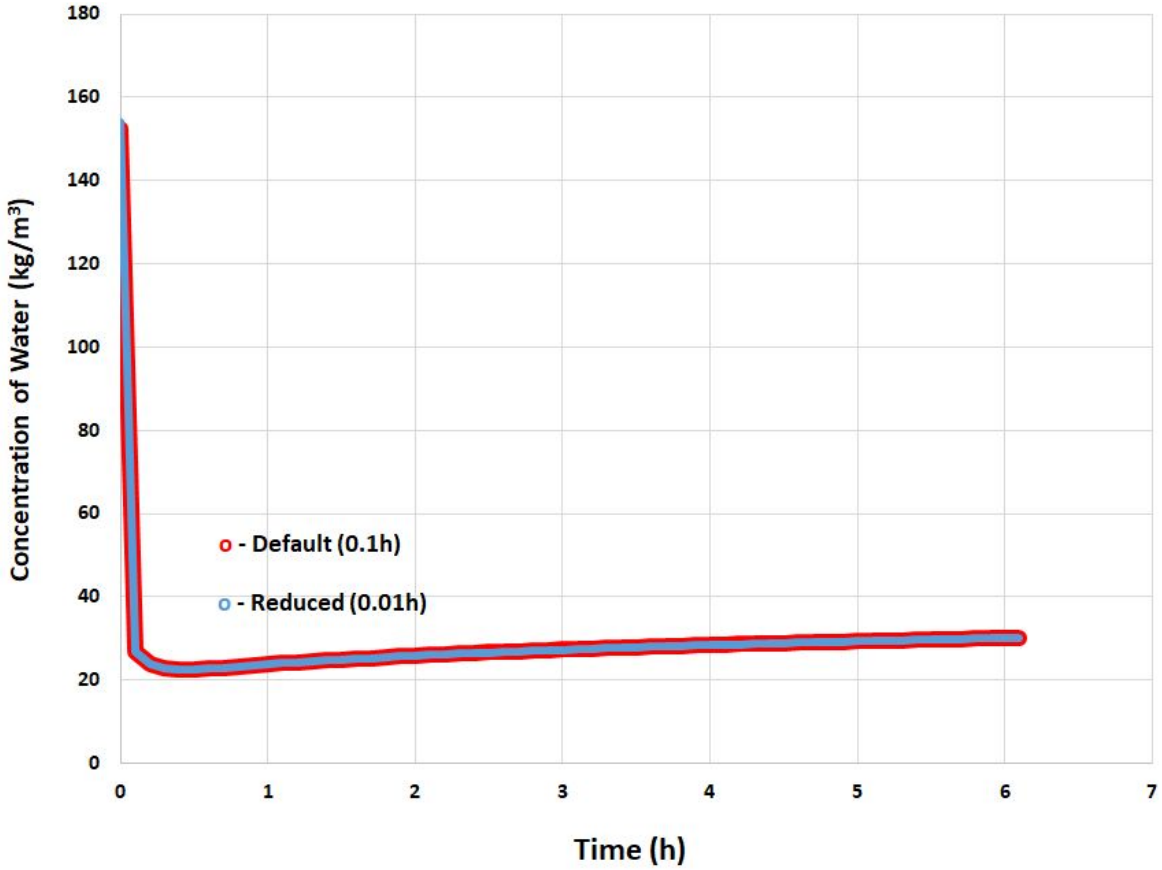

Fig. 4: **Average Water Concentration Near the Wound Surface Over Time for Varying Time Steps**: Depicted are two lines for a maximum time step of 0.1 h (labeled "Default") and 0.01 h (labeled "Reduced"). Please note that the solution curves are overlaid on one another. The line thicknesses in this graph are varied to allow the depiction of both solutions simultaneously.

As can be seen from the results above, the decrease of the default maximum time step by an order of magnitude did not produce any observable difference in average concentration computed. The solutions of the model for the varying time steps are nearly identical and are overlapping for all times. This suggests that the solution has converged to a value above the default value of 0.1 h and that the default value of time step is sufficiently small to avoid time-discretization error. Thus, a time step value of 0.1 h was implemented in this model.

4.3 Mesh Convergence:

Discretization error must also be addressed in the spatial dimension, thus mesh convergence was performed. The model was run for varying mesh densities to observe the effect the mesh density had on the computed solution. This variation in mesh density only occurred in the dermis (with an exception of the region just below the wound surface), epidermis, hydrocolloid, and polymeric barrier layer. The stratum corneum and region of the dermis nearest the wound surface were kept at a high mesh density due to the high concentration gradients in these regions. For further explanation, refer back to *Section 4.1*.

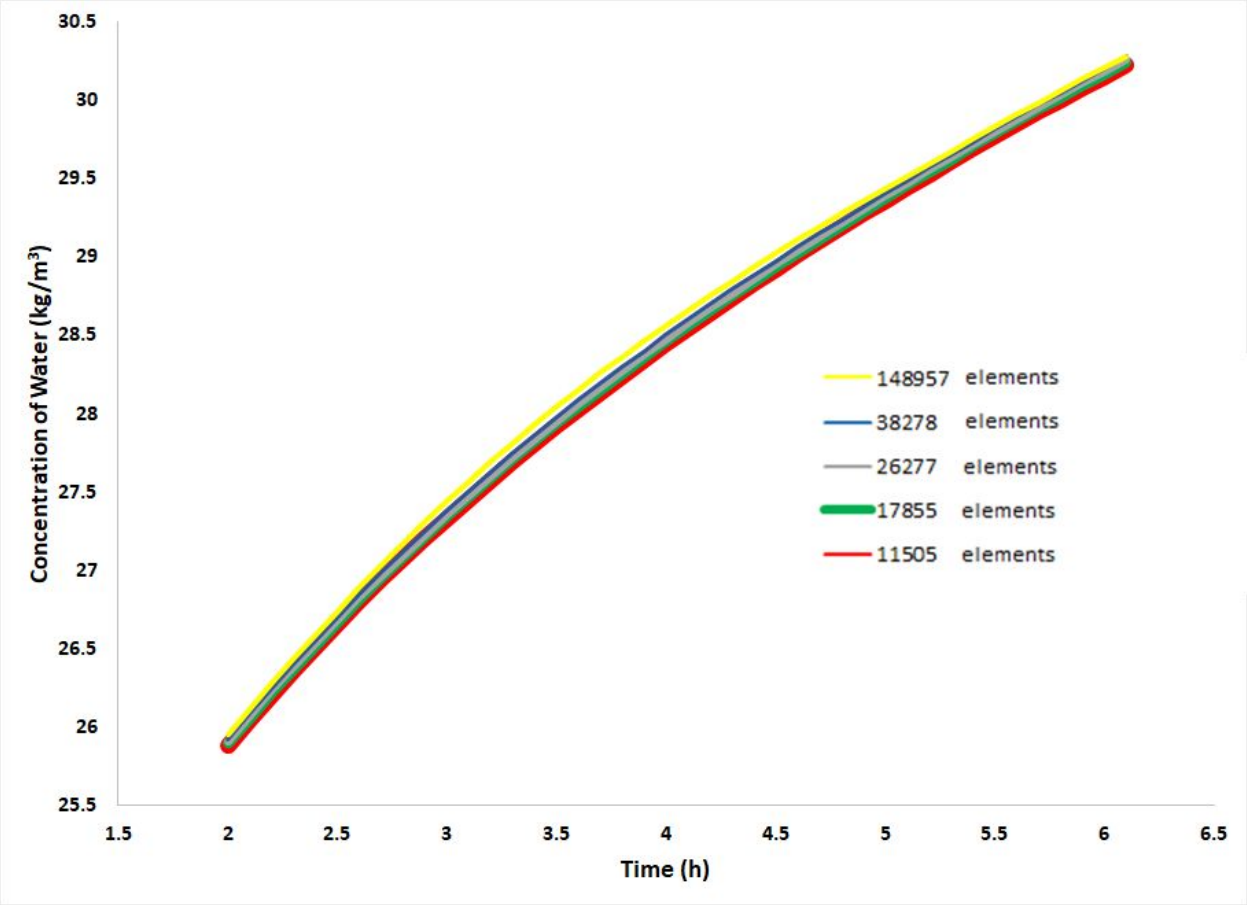

Fig. 5: **Average Water Concentration at Region Near the Wound Surface Over Time for Varying Meshing Densities**: The solutions are extremely similar and the line thicknesses were varied to allow for the depiction of all mesh densities on one plot. Please note the scale of the y-axis and the times this measurement was taken.

Illustrated above, mesh convergence was performed by varying the meshing densities, ranging from ~11,000 elements to ~149,000 elements. There is no discernable difference in the results as the mesh is refined to higher densities, suggesting that the solution converges at a relatively low mesh density.

It is important to note here that this convergence is not observed for very early times in the model. As depicted below in *Figure 6*, solutions in the early times (0-0.1h) had noticeable variation in average concentration that was computed.

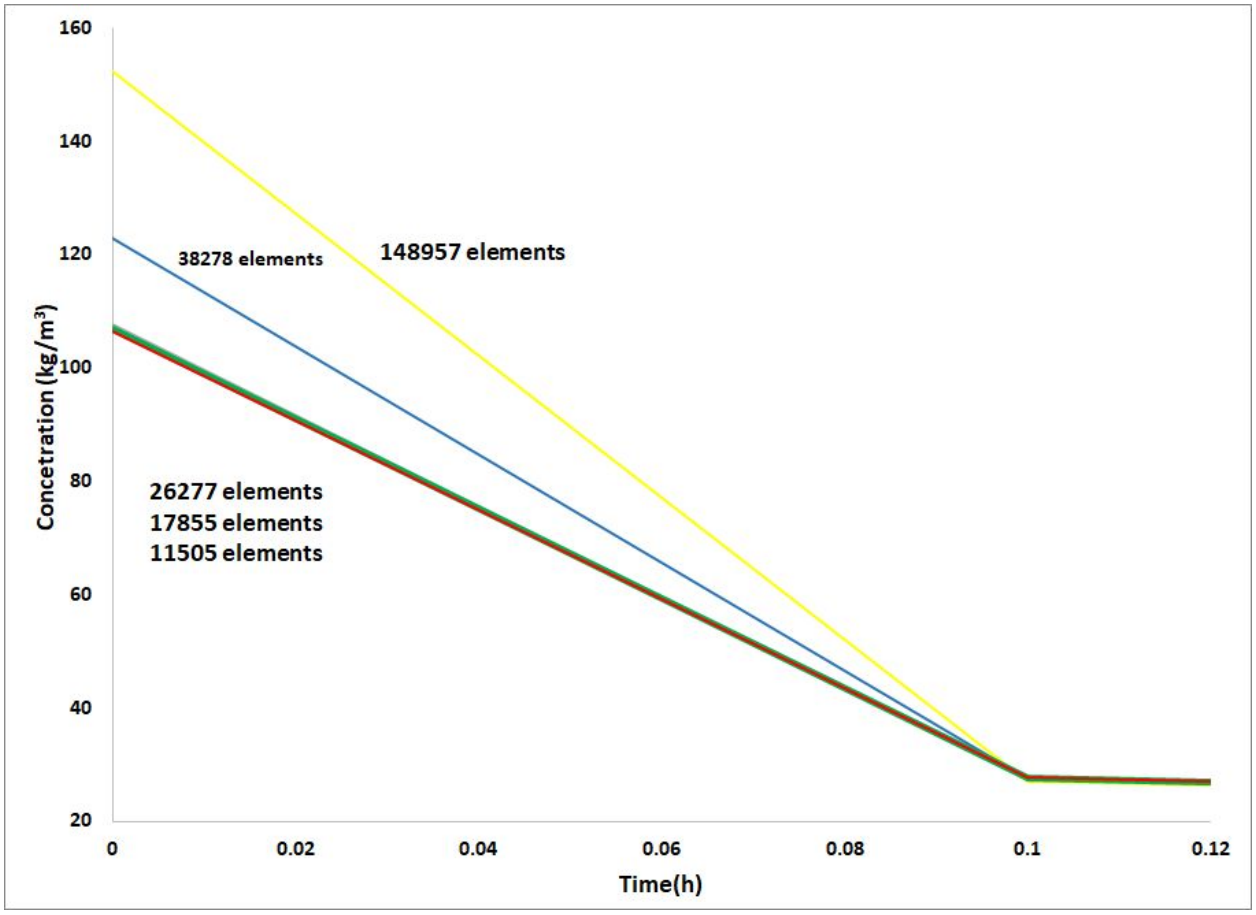

Fig. 6: **Average Water Concentration at Region Near the Wound Surface Over Time for Varying Meshing Densities, Early Times:** Take notice of the variation in initial average water concentration computed at time zero and the convergence of solutions at time 0.1 hours. Solutions computed with 11,505-26,277 elements were nearly identical and difficult to resolve on the same plot.

The type of variation between solutions that is seen above is something that results from spatial discretization errors; however, this type of error is insignificant considering that this model is only concerned with later times in the transport processes when the model has met a sort of quasi-equilibrium. *Figure 5* confirms that for the time ranges of interest to the investigation, the model has converged to a solution for the given mesh densities used. Mesh Convergence was evaluated over the domain shown in *Figure 7* below.

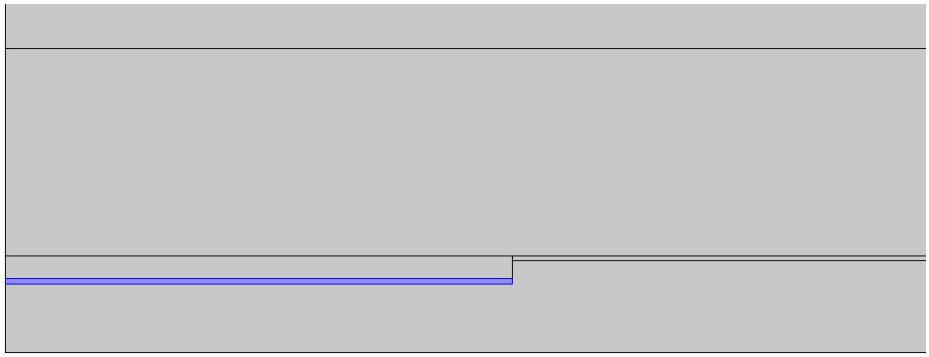

Figure 7: **Domain Used to Perform Convergence Analysis**

Fig. 7: shown above provides a pictorial description of the area over which mesh convergence was analyzed. A surface average of the concentration of water in this area was used to determine mesh convergence because this domain holds great relevance for the problem formulation. Specifically, this domain influences both the ability of the hydrocolloid to retain moisture as well as the ability of the skin to maintain physiological water content.

4.4 Validation:

In order to confirm that the model realistically depicts the transport phenomena of interest, the model was compared to experimental measurements available for water concentration in human skin and rates of water transport in wounded porcine and human skin.

Water concentration across human skin depth *in vivo* was experimentally measured and compared with the water concentration profile of the model shown in *Figure 8* [8].

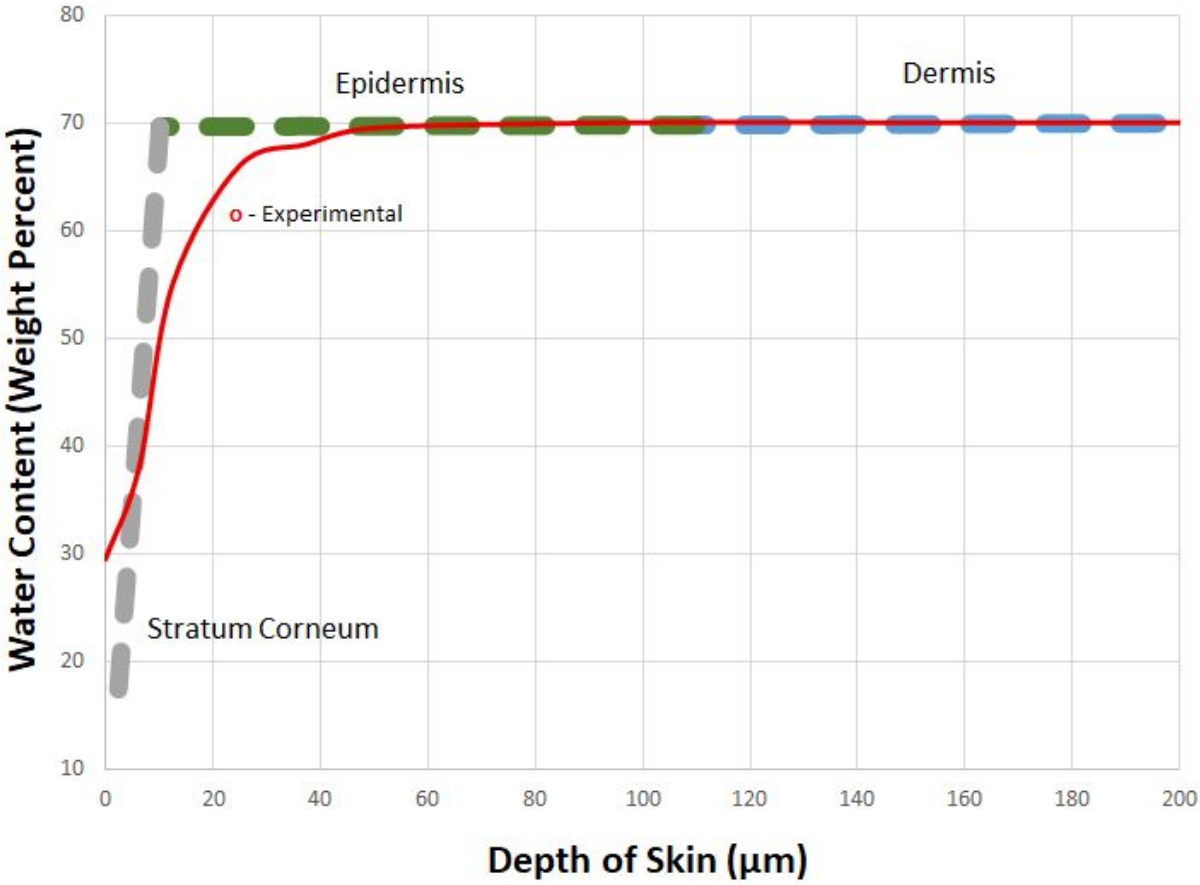

Fig. 8: **Model Generated Depth Profile of Water Concentration at Time 6 Hours Compared to Experimental Water Profile:** Similarities can be drawn between the measurements made by Nakagawa, Noriaki, et al (seen in red) and the model generated water concentration profile (multicolored) [8] .

The depth profiles pictured above share very similar trends in concentration through the skin depth. The clear parallels that exist between the depth profile generated by the model and the depth profile measured experimentally provide some support that our model is physically realistic.

Other experimental data exists to provide further points of comparison for the model. The TEWL of burn patients was measured clinically and the TEWL of wounded porcine skin was also measured [21][7]. These measurements can be compared with the TEWL of the model, as shown below in *Figure 10*.

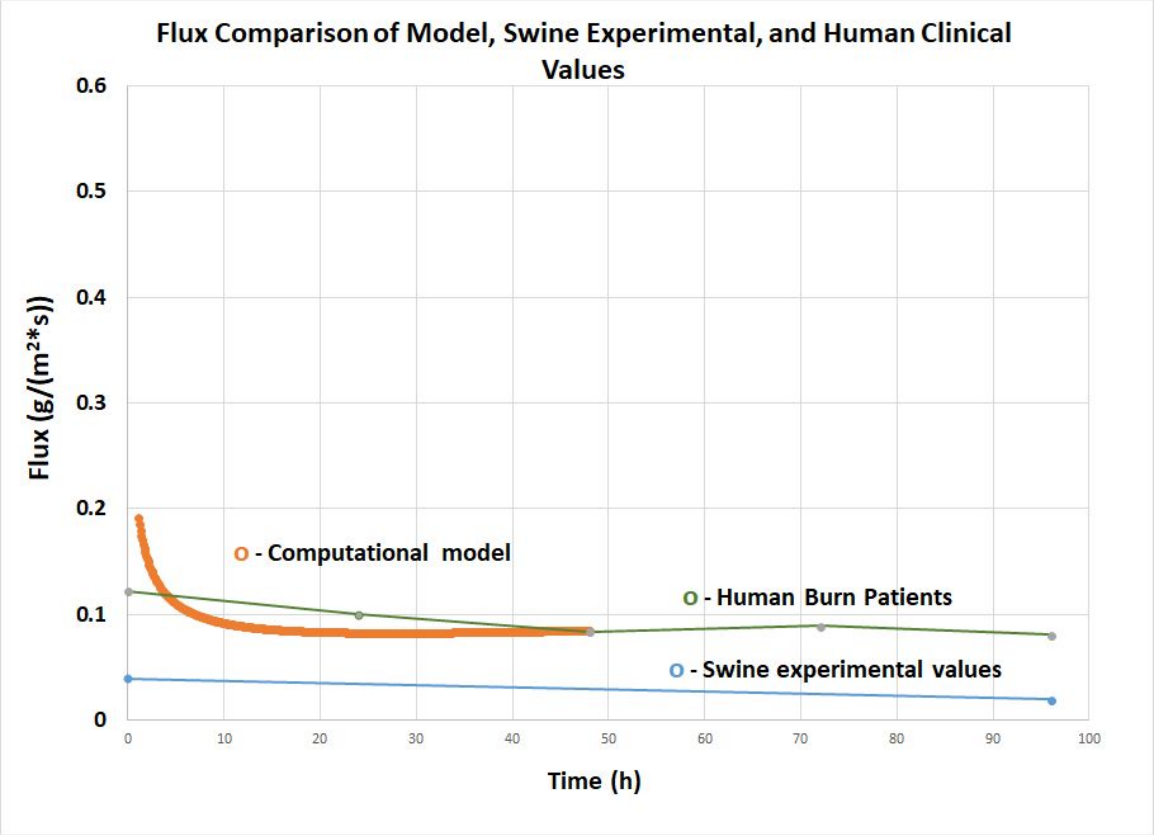

Fig. 9: **TEWL (Water Flux) of Several Wounds**. The computational model value for average TEWL through the wound surface over time is compared with a swine model for a partial-thickness wound and human burn patients. Measurement was made via an evaporimeter[7],[21].

The first TEWL used for reference was experimentally measured by Pirone et. al., where measurements of water vapor flux were taken directly above a partial-thickness wound in a porcine model after removal of a wound dressing and a waiting period to allow for any accumulated exudate to evaporate off [7]. Pirone et. al. were interested in the effects that different types of dressings had on the wound healing process and specifically measured the differences in TEWL (synonymous to WVTR) at various points in the healing process, as seen in *Fig. 10*. For the interest of validation, the flux values of the computational model were compared to those in Pirone's study because they used DuoDERM® CGF as a wound dressing in their study and because porcine skin models are considered excellent analogues to human skin [20]. The second reference TEWL that was of interest came from measurements of clinical burn wound patients [21]. Patients presenting with 2nd-3rd degree burns were kept in similar temperature and relative humidity conditions to those of our model, and the TEWL of these patients was taken once per day [21]. Opon comparison of the model with these experimental measurements, one can see similarities in the values of and trend in flux over time. This furthers the models validity as a model of skin water transport phenomena.

The two sets of comparisons between the model and measured experimental values presented provides strong evidence that the model has a basis in reality for the depiction of the quantities of interest.

5.0 Results

The results of this computational model suggest that DuoDERM® CGF has the ability to effectively sequester moisture above the wound bed, but it also demonstrates that the dressing is not able to effectively maintain physiological skin water content because it allows too much water to escape the wounded tissue. More specifically, analysis of the skin water content when treated with DuoDERM® CGF shows that much of the skin falls below physiological water contents, which would ultimately impair the healing process. To objectively quantify the performance of the dressing, an objective function was implemented. Further, a sensitivity analysis was performed to both verify prior assumptions as well as to delineate the important parameters of the scenario being modelled. Using both the objective function and the results from the sensitivity analysis, design recommendations were made regarding the material properties for an improved hydrocolloid dressing. This optimal solution will be analysed and its implications for future dressing design will be discussed.

5.1 DuoDERM® CGF Analysis:

The simulation of the DuoDERM® CGF hydrocolloid wound dressing revealed that the hydrocolloid dressing was able to fulfill its design specification: to absorb and hold wound moisture. An overall plot of the water profile following six hours of simulation with the DuoDERM® CGF hydrocolloid wound dressing can be seen in *Figure 11* below. A more in-depth analysis of this plot follows.

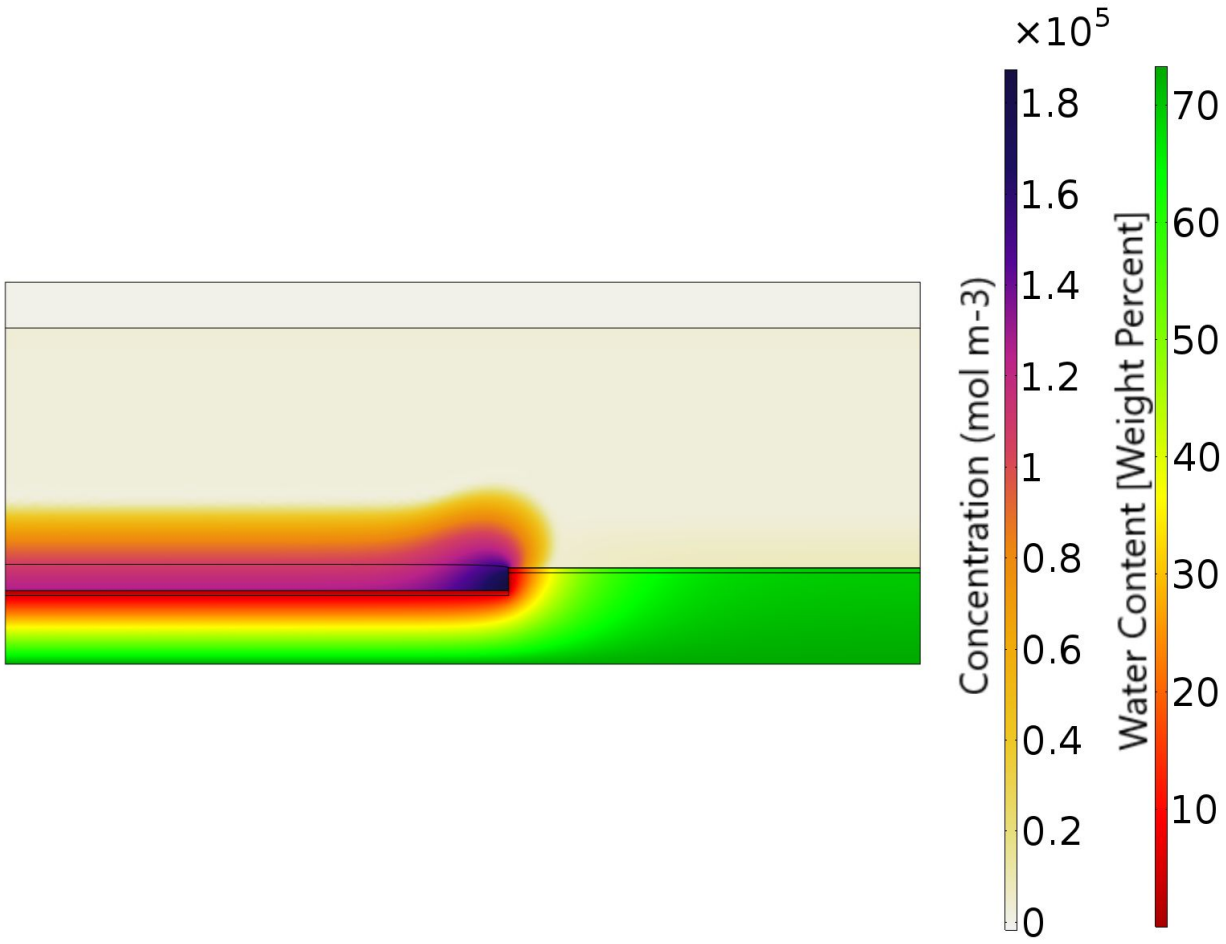

Fig. 10: **Concentration Profile of Simulated DuoDERM® CGF after 6 Hours**

From *Figure 11* above, it can be seen that water escapes the wounded tissue and is sequestered in the hydrogel. Both of these results are expected: wounded tissue should lose water, and the hydrocolloid, per its design specification, should retain this water. In order to visualize these phenomena in an in-depth and separate manner, the two results were isolated and their individual analysis can be seen in *Figures 12* and *13* below, where *Figure 12* shows the water content in the skin relative to physiological water content and *Figure 13* shows the amount of water retained in the hydrocolloid area directly above the wound bed over time.

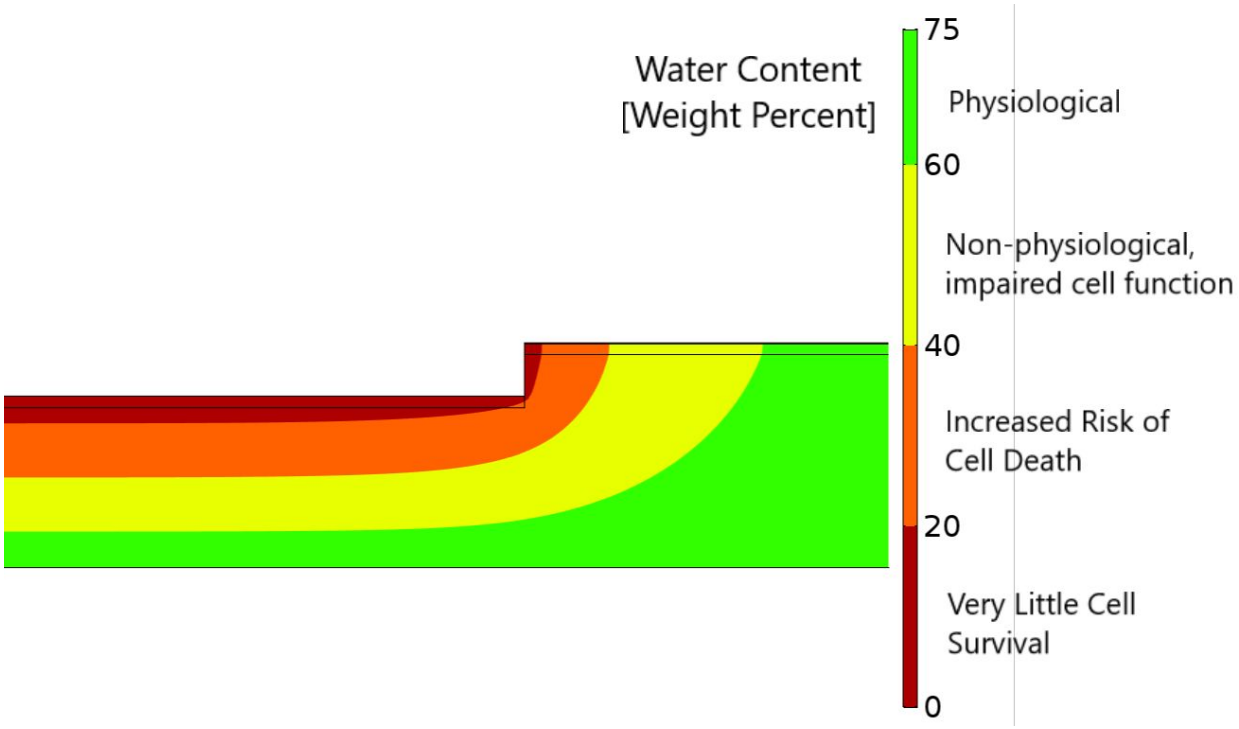

Fig. 11: **Water Content Profile in the Skin after 6 hours of Dressing Simulation:** The measured values of physiological water contents are related to their expected outcomes.

The area in *Figure 12* above, corresponding to 60-75% water content, signifies tissue within physiological ranges of water content. Between 40-60% water content signifies tissue with non-physiological water content, which will cause impaired cell function. Between 20-40% water content will cause increased cell death, and between 0-20% water content there will be very little cell survival. Based on these observations, the performance of the hydrocolloid dressing as it relates to maintaining skin water content near physiological levels was non-ideal. In fact, the majority of the simulated skin tissue below the wound falls below physiological levels of water content, and much of the tissue is even put at risk for increased cell death. This outcome is precisely poor for a wound dressing designed to retain moisture to facilitate wound healing. The amount of water retained in the hydrocolloid in the area directly above the wound bed was then calculated and can be seen in *Figure 13* below.

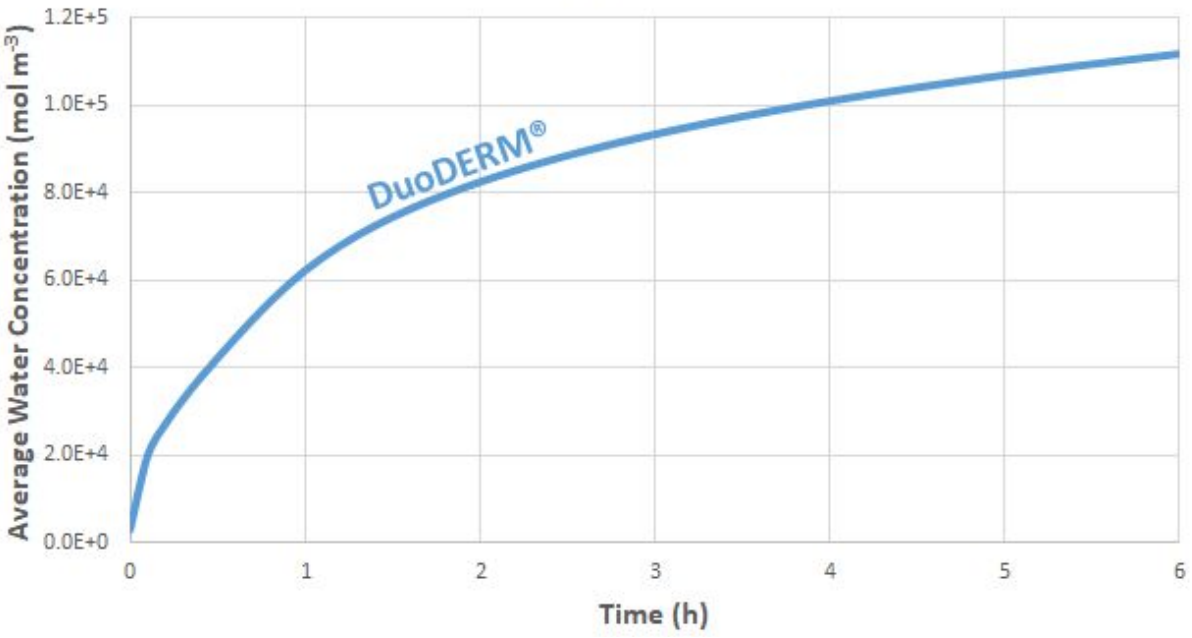

Fig. 12: **Average Water Concentration in Hydrocolloid Dressing above wound Surface over Time:** The domain in which this measurement was taken can be seen in *Figure 17*. Please refer to *Figure 21* to see the domain over which this average concentration was calculated.

As can be seen in *Figure 13* above, the hydrocolloid quickly absorbs moisture from the wound and retains that moisture in the area above the wound bed over a long period of time. This moisture in the hydrocolloid above the wound will facilitate cell migration, granulation, and re-epithelialization: all important factors in the process of wound healing. Based on these results alone, the hydrocolloid successfully promotes an environment conducive to wound healing; however, when these results are evaluated in conjunction with the levels of skin water content shown in *Figure 12* above, the hydrocolloid overall was deemed unsuccessful in its approach to wound healing.

Based on these tentative conclusions, an objective function was implemented to more completely quantify the performance of the hydrocolloid dressing. Then, a sensitivity analysis of the hydrocolloid was performed in order to determine what parameters would be best to alter in order to effect a more optimal solution. Finally, this optimized solution was simulated and compared to the implementation of the standard DuoDERM® CGF hydrocolloid wound dressing.

5.2 Objective Function:

The objective function is implemented with the rationale that it is best to maintain the dermis at its initial water concentration in order to prevent further damage to the tissue. The objective function also considers that the hydrocolloid should retain water near the surface of the wound bed in order to facilitate the migration of cells responsible for wound healing. With this result in mind, equation (12) below was implemented as an objective function to analyze the computational results.

$$\Omega = [(C_S - 1.15C_{S,0})(C_S > 1.15C_{S,0}) + (0.85C_{S,0} - C_S)(C_S < 0.85C_{S,0})] - (C_H - C_{H,0}) \qquad (12)$$

where Ω is the objective value, $C_{S,0}$ is the initial concentration of water in the skin, C_S is the concentration of water in the dermis and epidermis at the time of evaluation, $C_{H,0}$ is the initial concentration of water in the hydrocolloid and C_H is the average concentration of water in the hydrocolloid domain above the wound bed at the time of evaluation.

The function works by adding the concentration of all points within the dermis and epidermis that are 15% above or below the initial concentration of the dermis, which provides an objective measure of the ability of the hydrocolloid to maintain the skin at physiological water content. The second term in the equation, $(C_H - C_{H,0})$, provides an objective analysis of the hydrocolloid's ability to retain moisture in the domain above the wound bed. The first part of the objective function, $[(C_S - 1.15C_{S,0})(C_S > 1.15C_{S,0}) + (0.85C_{S,0} - C_S)(C_S < 0.85C_{S,0})]$, relates to the skin water content and should be minimized to zero in order to indicate the entire skin domain to be within 15% of physiological water content. The second part of the objective function should be maximized to indicate that the hydrocolloid is retaining a maximal amount of water in the area above the wound bed. The implementation of this objective function requires Ω to be minimized to obtain an optimized solution . Parameters that the model is particularly sensitive to were identified in the sensitivity analysis in order to create an optimized solution.

5.4 Sensitivity Analysis:

Parameters of the model, including the diffusivity of the hydrocolloid, diffusivity of the barrier layer, thickness of the hydrocolloid, thickness of the barrier layer, mass transfer coefficient of the convective flux, partition coefficient between the hydrocolloid and polymer barrier layer, partition coefficient between the skin and hydrocolloid, and the relative humidity were altered to test the model's sensitivity. All diffusivities and the partition coefficients were tested one magnitude above and below the control. The thicknesses and mass transfer coefficient of the convective flux were altered ± 10% .

The analysis was on the concentration and flux of a selection in the dermis right below the wound because this is the critical zone of interest. The analysis showed that hydrocolloid diffusivity and the partition coefficient between the skin and hydrocolloid to have large effects on the concentration and the flux on the wound surface. The diffusivity of the barrier layer and relative humidity had very small or no changes. The mass transfer coefficient of the convective boundary at the interface of the polymer barrier layer and air also had very small or no changes. The effect on the flux from the polymer barrier layer to air from altering any parameters were negligible. The thicknesses of the hydrocolloid and polymer barrier layer presented no effects to any of the concentration or flux profiles.

The most important parameters were the diffusivity of the hydrocolloid and the partition coefficient between the skin and hydrocolloid. The sensitivity for the parameters were assessed both with concentration and flux at the wound bed. The concentration profile taken underneath the wound surface inside the dermis is seen in *Figure 14 and 15* for the diffusivity of hydrocolloid and the partition coefficient, respectively. The flux profile taken at the wound

surface is seen in *Figure 16 and 17* for the diffusivity of hydrocolloid and the partition coefficient, respectively.

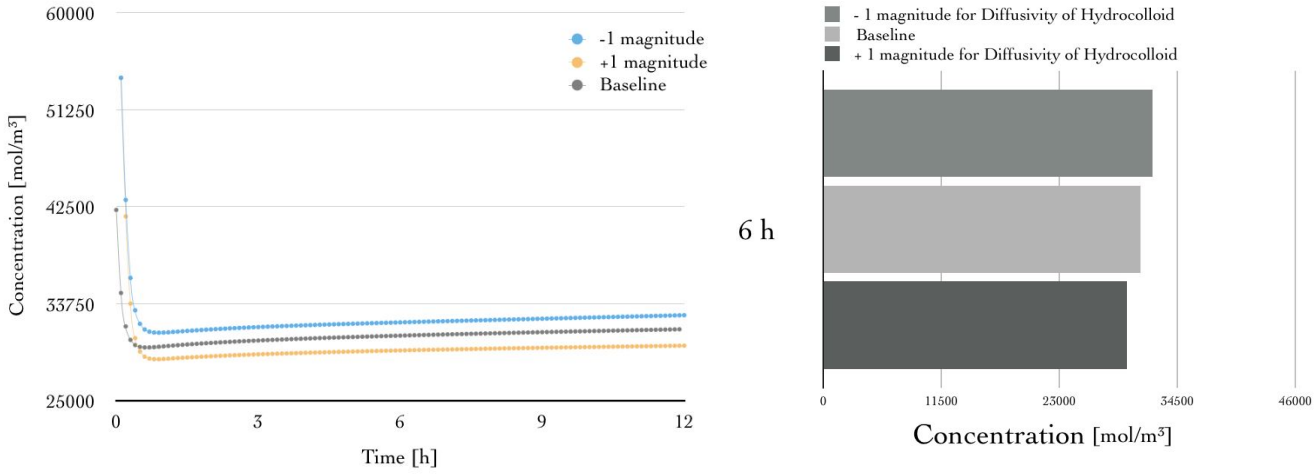

Fig. 13: **Concentration Profile for the Sensitivity Analysis of Hydrocolloid Diffusivity:** The magnitude of the diffusivity of the hydrocolloid was varied ± 1 magnitude in comparison with the existing value. These concentration profiles were taken underneath the dermis below the wound surface. [Left] The variance of concentration for this parameter over a 12 hour interval. [Right] The variance of concentration for this parameter at 6 hours.

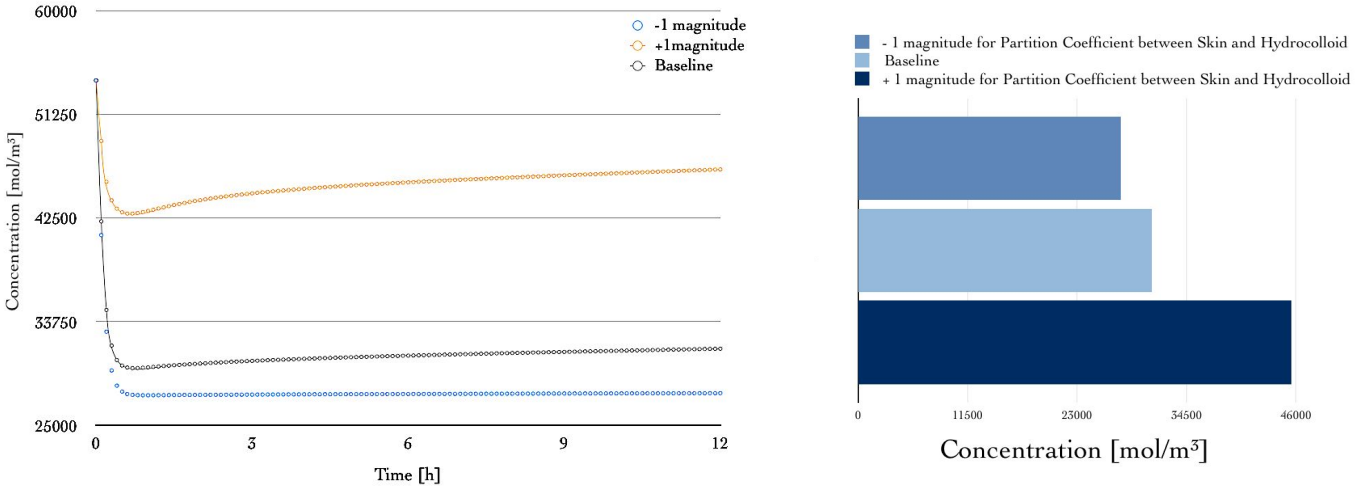

Fig. 14: **Concentration Profile for the Sensitivity Analysis of the Partition Coefficient between the Skin and Hydrocolloid:** The magnitude of the partition coefficient was varied ± 1 magnitude in comparison with the existing value. These concentration profiles were taken underneath the dermis below the wound surface. [Left] The variance of concentration for this parameter over a 12 hour interval. [Right] The variance of concentration for this parameter at 6 hours.

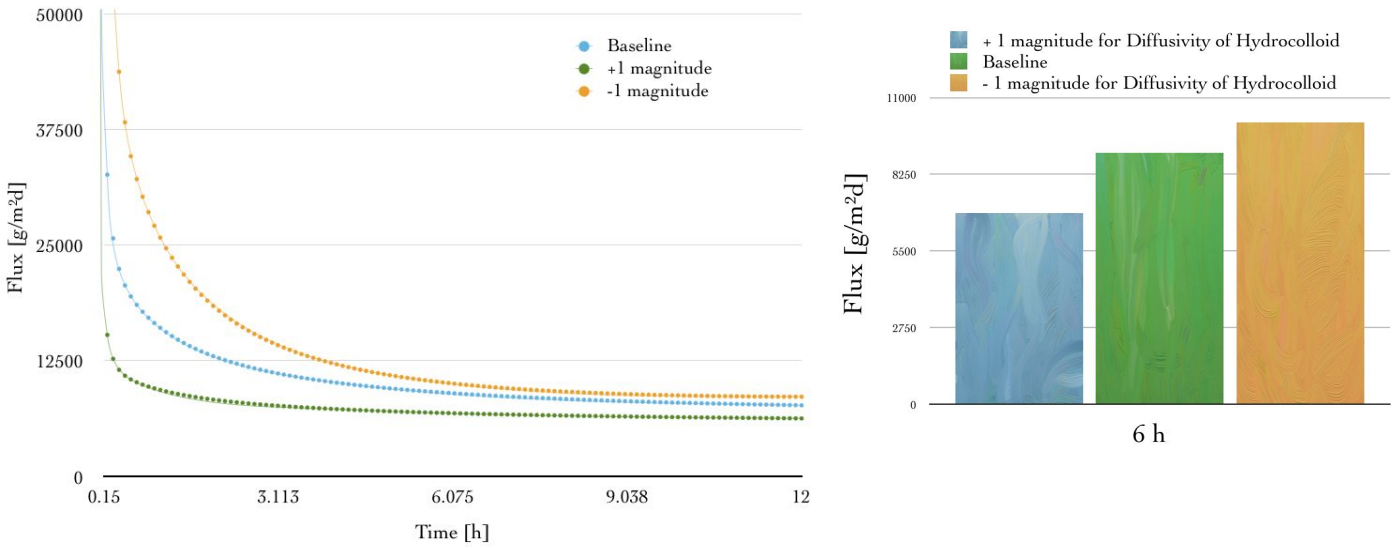

Fig. 15: **Flux Profile for the Sensitivity Analysis of Hydrocolloid Diffusivity:** The magnitude of the diffusivity of the hydrocolloid was varied ± 1 magnitude in comparison with the existing value. These flux profiles were taken at the wound surface. [Left] The variance of flux for this parameter over a 12 hour interval. [Right] The variance of flux for this parameter at 6 hours.

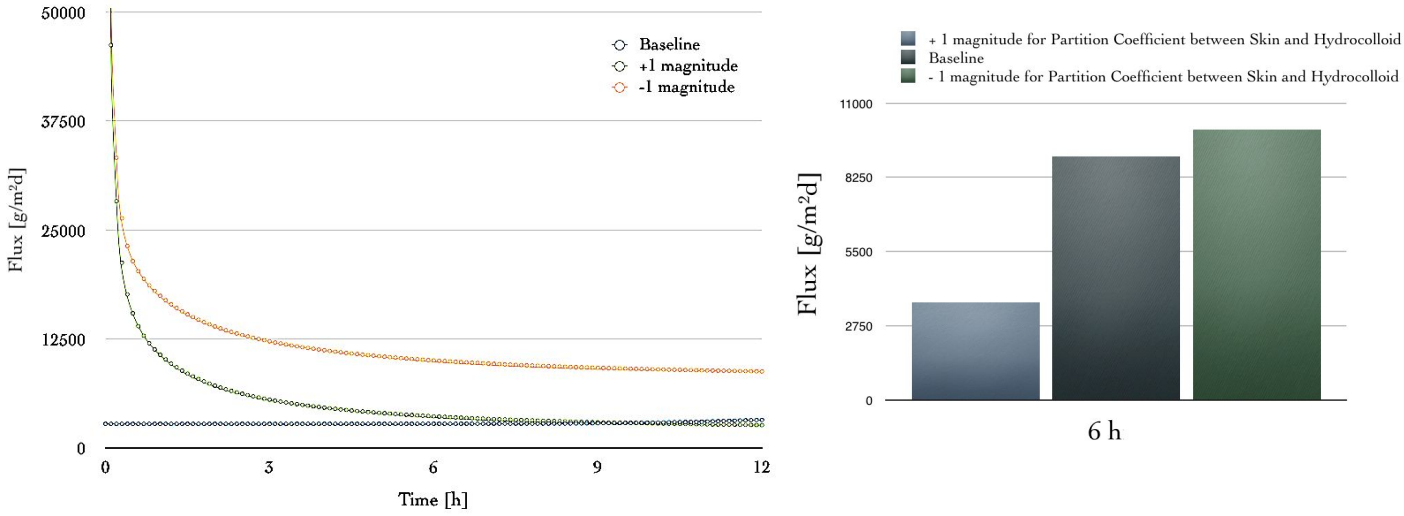

Fig. 16: **Flux Profile for the Sensitivity Analysis of the Partition Coefficient between the Skin and Hydrocolloid:** The magnitude of the partition coefficient was varied ± 1 magnitude in comparison with the existing value. These flux profiles were taken at the wound surface. [Left] The variance of flux for this parameter over a 12 hour interval. [Right] The variance of flux for this parameter at 6 hours.

The other parameters were negligible as they had very minimal changes to both concentration and flux. The data for the sensitivity analysis of the other parameters can be seen in *Section 8.4 Appendix D (Sensitivity Analysis of Other Parameters)*.

5.5 Optimization and Design Recommendation:

In order to optimize the design of the hydrocolloid wound dressing, it is important to minimize the objective function. In this minimization, the parameters that were altered were the diffusivity of the hydrocolloid and the partition coefficient between the hydrocolloid and skin. These two parameters were chosen because the hydrocolloid was the most sensitive to their influence. Further, both parameters are readily changeable material properties, so it makes sense to computationally alter them in order to inform future designs. The diffusivity of the hydrocolloid and the partition coefficient between the skin and the hydrocolloid were thus iteratively altered until the objective function was minimized. This resulted in a hydrocolloid with a 50X reduction in diffusivity and a 10X reduction in partitioning compared to the original DuoDERM® CGF values.

To evaluate this optimized solution, it was compared to the original solution based on its abilities to maintain the skin at physiological water content and to retain moisture near the wound bed. The complete solution using the optimized values for partition coefficient and diffusivity in the hydrocolloide as seen in *Figure 18* below.

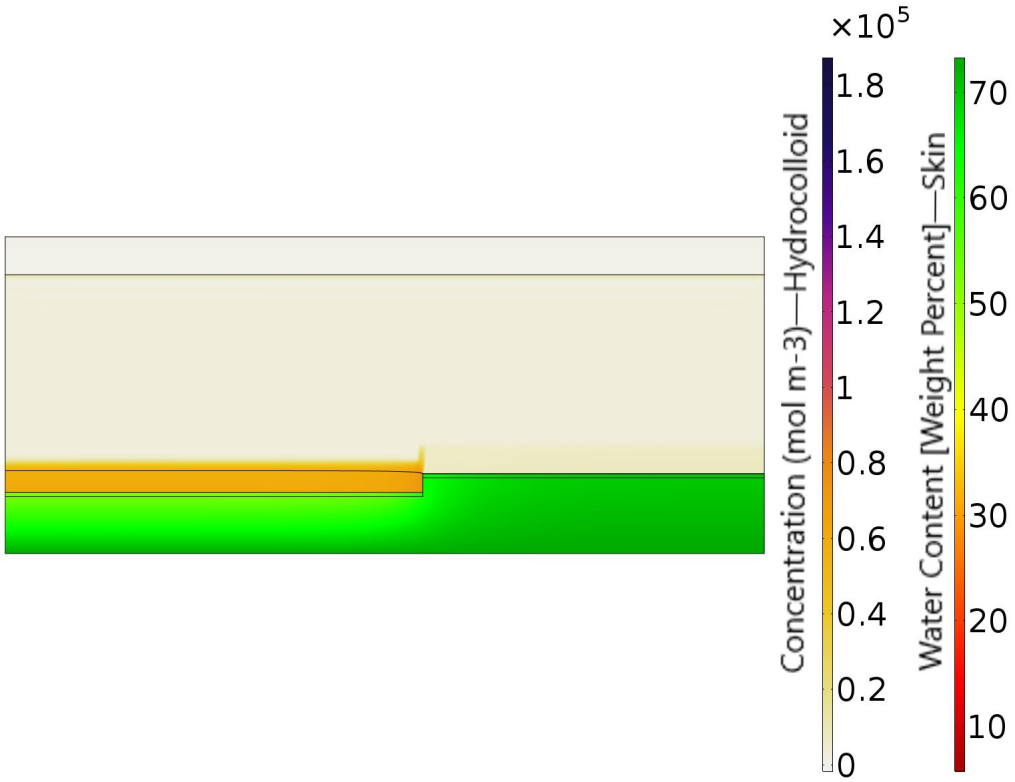

Fig. 17: **Water Concentration Profile of optimized design after 6 hours of Simulation:** Depicted is an optimized water concentration profile in the skin and hydrocolloid domains.

Compared to the original results shown in *Figure 11*, these optimized results clearly show that this implementation does a better job of maintaining the skin at physiological levels of water content. This implementation does not, however, retain as much moisture in the domain above the wound bed. The ability of this optimized solution to maintain physiological levels of water content compared to the original solution is investigated more thoroughly in *Figure 19* below.

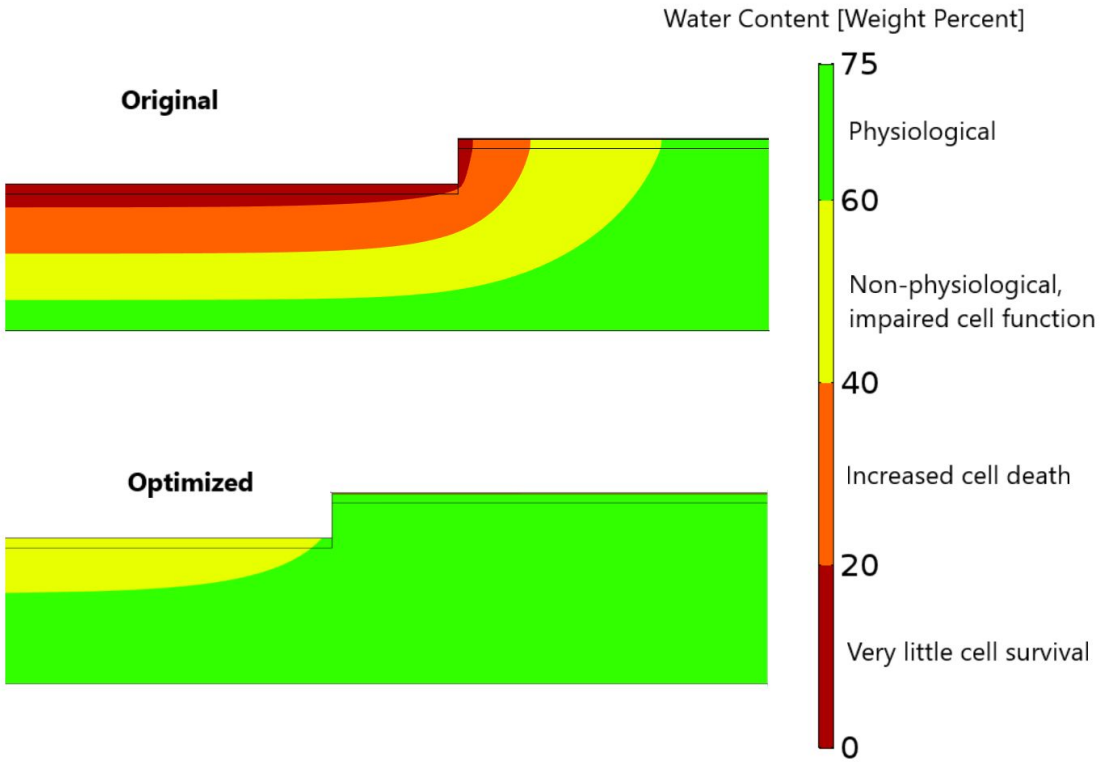

Fig 18: **Comparison of Skin Water Content in Original and Optimized Simulations:** Skin water profiles for the original and optimized wound dressing formulation.

As can be seen in *Figure 19* above, the optimized solution maintains significantly more of the skin at physiological levels of water content, with no part of the skin at risk of increased cell death. This signifies a much better overall solution compared to the original implementation where more of the otherwise healthy skin domain will die as a result of the hydrocolloid wound dressing. The other specification of interest, the ability of the hydrocolloid to retain moisture above the wound bed, was compared between the original and optimized solution in *Figure 20* below.

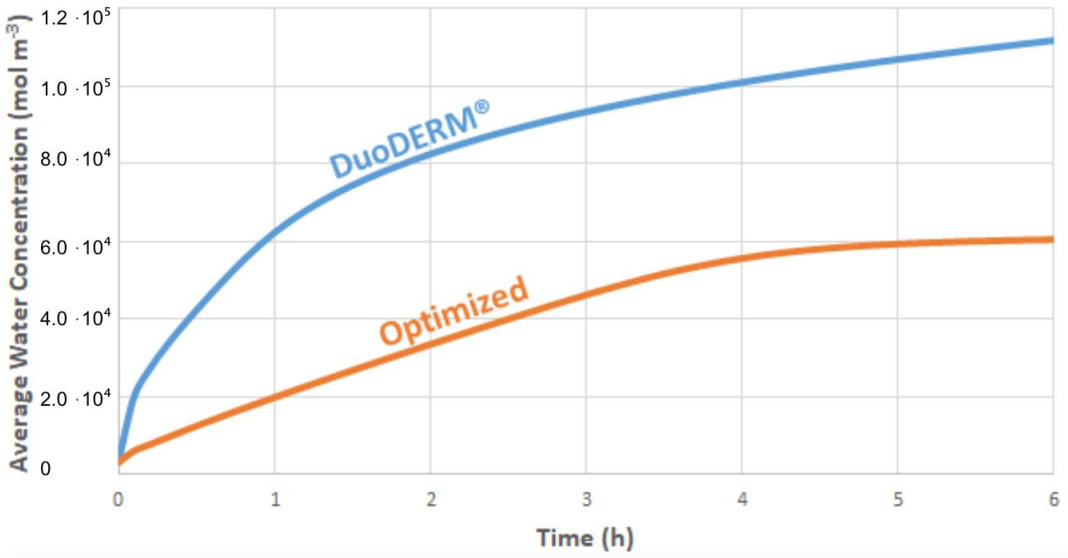

Fig 19: **Comparison of hydrocolloid water retention in domain Above the Wound**: The domain in which this measurement was taken can be seen in *Figure 21*.

As can be seen in *Figure 20* above, the optimized hydrocolloid design does not retain as much moisture above the wound bed as the original hydrocolloid implementation does; however, this result is trivial in comparison to the optimized hydrocolloid's ability to maintain the skin at physiological levels of water content. Further, the optimized solution is still able to retain some water above the wound bed, which will still aid cell migration and contribute to a faster healing process while preventing additional cell death in the skin.

Overall, the optimal solution provides great advantages over the current implementation of DuoDERM® CGF because of its greatly improved ability to maintain the skin at physiological levels of water content. The lower partition coefficient of the optimized design informs future wound dressing designs to be more hydrophobic. Further, the lower diffusivity of the optimized design informs future dressings to provide more diffusive resistance to water.

Figure 21 below shows the domain that was used to measure the hydrocolloid's ability to retain moisture in the area above the wound bed.

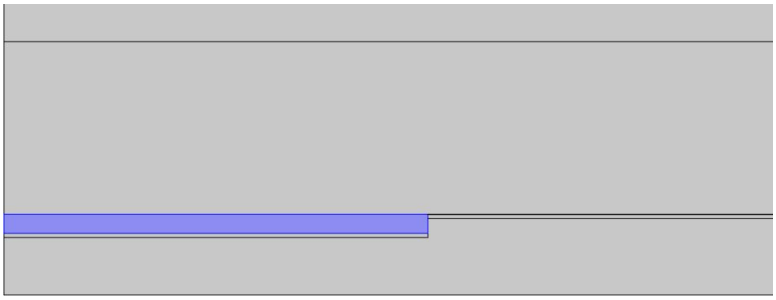

Figure 20: **Domain in which Hydrocolloid Water Retention was Measured**

To perform this measurement, a surface average of concentration was evaluated over this domain and plotted over time, which can be seen in *Figures 20 and 13* above.

6.0 Discussion

The results of this study suggest using wound dressings that are more hydrophobic and create more diffusive resistance for water. These results are incredibly interesting, especially in comparison to current wound dressing paradigms. It is important to consider, however, the limitations of the model used to derive these solutions. It is also important to consider potential future additions for this model, which serve as a basis and proof-of-concept for the modelling of water transport in hydrocolloid wound dressings.

6.1 Limitations:

Water transport in the skin is implemented in this model as diffusion in porous media as described in equation (1). In addition to diffusion in porous media, water in the skin flows as a result of interstitial pressure gradients [15]. Importantly, these pressure gradients are lost or reduced in response to partial- and full-thickness wounds that damage the integrity of the stratum corneum [16]. Water also flows in the skin as a result of osmotic pressure gradients, where the concentration of ions throughout the skin must be considered. These ions are also transported in the interstitial fluid of the skin, so the response of overall water transport in the skin must be a fully coupled solution of water and ion transport as described by van Kemanade in her 1998 thesis [12], which this model did not implement. Further, water is perfused into the dermis and hypodermis from blood vessels and capillaries as described in the Starling Hypothesis [17].

The swelling of the hydrocolloid, in this model, was implemented as a time-dependent velocity in the hydrocolloid layer using the *Deformed Geometry* module in COMSOL®. A more accurate implementation of swelling would be dependent on local water concentration described empirically. This would be implemented using the COMSOL® module *Moving Mesh*, which implements an Arbitrary Lagrangian-Eulerian (ALE) method.

Further, this model is only capable of modelling partial-thickness wounds because the geometry only extends to the bottom of the dermis. In order to model deeper wounds and more accurately model partial-thickness wounds, deeper layers of the skin such as the hypodermis should be included in the model.

6.2 Additional Suggestions:

This model, as it is currently implemented, models only one component of the many complex elements involved in wound healing. Fortunately, the model is also fairly easy to modify. As such, it would be interesting to include additional components of healing in this model in order to understand how the hydrocolloid wound dressing influences healing in ways other than influencing water transport. For instance, autolytic degradation can be modelled to understand how the hydrocolloid influences the ability of the skin to remove dead tissue. Further, chemokine factors can be modelled to understand how the hydrocolloid influences the propensity of a wound for chronic inflammation versus wound healing. In fact, some hydrogel wound dressings are specifically designed to sequester certain chemokines in order to promote wound healing in chronic wounds, such as those found in diabetes and chronic leg ulcers [18]. In addition, cellular deposition and re-epithelialization can be modelled in order to see how the hydrocolloid influences the entire wound healing process.

6.3 Future Direction:

Although this model provides great insight into the design of next-generation wound dressings, it is necessary to validate these results *in vitro* before applying them toward clinical applications. Further, the investigation of additional hydrocolloid parameters could provide additional insight into the design of next-generation wound dressings, aside from just partitioning and diffusivity. These suggestions would be good to understand before pre-clinical and clinical testing to ensure an optimal design. Finally, it would be interesting to see how functional modification of hydrocolloid and hydrogel dressings, such as the inclusion of sequestered heparin, influence the results of this study in an experimental setting.

7.0 Conclusion

Hydrocolloid and hydrogel wound dressings are attractive materials for wound dressings because of both their ability to absorb large amounts of wound exudate as well as their modularity of design. Hydrogels and hydrocolloids, with regard to their use as wound dressings, can occasionally lead to excess drying of wounds, especially those that produce little exudate [19]. This computational model validates these observations by demonstrating that a hydrocolloid wound dressing, DuoDERM® CGF, is unable to maintain the skin at physiological levels of water content. In investigating the design of this hydrocolloid, it was found that the partitioning of water in the hydrocolloid was to blame for its inability to maintain physiological water contents. Further, it was determined that the diffusivity of water in the hydrocolloid caused less water overall to be retained near the wound bed. By lowering the diffusivity of water in the hydrocolloid and decreasing its partitioning of water relative to the skin, an optimal solution was created that both maintains the skin at physiological levels of water content and retains moisture near the wound bed. These results inform the design of future wound dressings. The next-generation of wound dressings should be:

1. More hydrophobic in order to decrease their partitioning of water relative to the skin.

2. Less diffusive with regard to water in order to retain moisture near open wound beds.

With these simple alterations, hydrocolloid and hydrogel wound dressings can be retained for their modularity by simply altering some of their defining physical properties. These changes can be as simple as increasing the number of lipid motifs in these materials and decreasing their average porosity. Overall, the results of this computational model suggest a paradigm shift in the construction of hydrocolloid and hydrogel wound dressings in a more hydrophobic and less diffusive direction.

8.0 Appendices

8.1 Appendix A (Input Parameter and Sources)

Table 1: **Layer properties and Initial Conditions for Computational Model**

Layer	Diffusivity [cm^2/s]	Temperature [K]	Porosity	Density [kg/m^3]	Initial Concentration [kg/m^3]	References
Stratum Corneum	$5 \cdot 10^{-10}$	310.15	0.1	1050	363.06	[4, 24, 27, 8]
Epidermis	$5 \cdot 10^{-6}$	310.15	0.3	1050	975.12	[4, 24, 25, 8]
Dermis	$2 \cdot 10^{-6}$	310.15	0.3	1050	975.12	[4, 24, 25, 8]
Polymer Layer	$2.3 \cdot 10^{-6}$	293.15	N/A	1120	18.88	[6]
Wound Dressing	$D(c) = (0.2147 + 3.372 \cdot 10^{-7} + 1.527 \cdot 10^{-6}c^2) \cdot 10^{-11}$	293.15	N/A	N/A	44.42	[6, 9]

Table 2: **Computational Model Variables**

Parameter	Definition	Value	References
C_{wpor}	Concentration of water in the skin layer	Varies with time and space [mol/m^3]	
C_{wcol}	Concentration of water in the hydrocolloid layer	Varies with time and space [mol/m^3]	
C_{wpol}	Concentration of water in the polymer barrier layer	Varies with time and space [mol/m^3]	
C	Universale water concentration value	Varies with time and space [mol/m^3]	
K_{sc}	Partition coefficient between the skin/wound and the hydrocolloid	$6.306 \cdot 10^{-2}$	[14]
K_{hp}	Partition coefficient between the hydrocolloid and the polymer (given as a function of concentration of water in the hydrocolloid, Cwcol)	$((0.226 \cdot \exp(5.836\ 10^{-4}[m^3/mol] \cdot C_{wcol})-0.206) /1.05\ 10^{-2})$	[6]
Radius	The radius of the area being studied	20mm	
RH	Relative humidity in the air environment	0.5	
T_{abs}	Room temperature	293 [K]	
MW_{water}	Molecular weight of water	18.01528 kg/mol	
BodyTemp	Body temperature	310.15 [K]	
ρ_W	Molar mass of water	18 g/mol	
D_{vair}	Diffusivity of water vapor in air	$0.256\ 10^{-4}\ m^2/s$	[28]

P_d	Partial pressure of dry air	$p_d \cdot (287.058\ [J/kg\text{-}K] \cdot T_r[K])$	[22]
P_v	Partial pressure of water vapor @20°C	$p_v \cdot ((461.5\ [J/kg\text{-}K]) \cdot T_{r[}K])$	[22]
ρ_d	Density of dry air @°20C	1.2041 [kg/m^3]	[22]
P_v	Density of water vapor @20°C	17.3 [g/m^3]	[22]
T_r[K]	Room Temperature in Kelvin	T_{Room} + 274.15 [K]	
R_u	Universal gas constant	8.3144598 [J/mol-K)]	
M_d	Molecular mass of dry air	0.028964 [kg/mol]	[22]
M_v	Molecular mass of water	0.018016 [kg/mol]	
g	Gravitational Constant	9.81 [m/s^2]	
u	Viscosity of water	$u_0 \cdot (493.47 \cdot T_{Room}/T_0)^{1.5} \cdot (T_0+198.72)/(493.47 \cdot T_{Room}+198.72)$	[23]
u_0	Viscosity of air at T0	17.83 10^{-6} [kg/(m-s)]	[22]
PerToCon	Converts Percentage Water Content to Concentration	1330 [kg/m^3]/MW_{water}	
K_{sc}	Partition Coefficient of the Stratum Corneum to Pure Water	6.306 10^{-2}	[14]
P_{tot}	Ambient moist air pressure	101325 [kg/(m-s^2)]	
VP_w	Vapor pressure of water at 20C and 1 atm	2366.7 [kg/(m-s^2)]	[22]
PP_w	Partial pressure of water at varying relative humidities	$RH \cdot VP_w$	[22]
V(t) or $an_i(t)$	Swelling Velocity of the Hydrocolloid	(3.7-2.206 10^{-5}t) $\cdot 10^{-8}$ [m/s]	[6]
ρ_{BL}	Density of the polyurethane barrier layer	1,120 kg/m^3	[6]
$S_{hydrocolloid}$	Solubility of the hydrocolloid	$0.226^{(5.836 \cdot 10^{-4})c} - 0.206$ [s^2/m^2]	[6]
$S_{barrier\ layer}$	Solubility of the barrier layer	$1.050 \cdot 10^{-2}$ [s^2/m^2]	[6]

8.2 Appendix B (CPU Runtime and Memory Usage)

Typical run metrics:

Solution time: 2337 s. (38 minutes, 57 seconds)
Physical memory: 2.85 GB
Virtual memory: 3.24 GB

8.3 Appendix C (Calculations)

[1] Mass Transfer Coefficient (h_m): Assuming flat horizontal plate, natural convection, and $T_s > T_\infty$

[13] $h_m = \frac{D_{AB}}{L} \cdot 0.54[(\frac{\mu}{\rho D_{AB}})(\frac{g\rho\Delta\rho_A L^3}{\mu^2})]^{1/4}$, where

A = water in the barrier layer
B = water vapor in air
D_{AB} = diffusivity of A into B = 0.257 cm^2/s at 20°C, and
L = Radius
μ = viscosity (Pa s) of air

[28]Sutherland's Formula: $\mu = \mu_0 \left(\frac{T}{T_0}\right)^{1.5} \left(\frac{T_0 + 198.72}{T + 198.72}\right)$, where

T_0=518.7 Rankine and
$\mu_0 = 3.6 \cdot 10^{-1}$ kg s/m^2 = $17.83 \cdot 10^{-6}$ N · s/m^2

[22] ρ = density of air = $\frac{Pd \cdot Md + Pv \cdot Mv}{RT}$, where

Pd is the partial pressure of dry air,
Md is the molar mass of dry air,
Pv is the partial pressure of water vapor,
Mv is the molar mass of water vapor,
R is the universal gas constant, and
T is temperature.

$\Delta\rho_A$ = the change in density of the water vapor from the surface - the water vapor in the ambient medium
g = gravitational constant

$$hm = \left(\frac{D_{v,air}}{Radius}\right) \cdot 0.54 \cdot \frac{gp_{air}\Delta\rho R^3}{u^2} \left(\frac{u}{p_{air} D_{v,air}} \bullet \frac{gp_{air}\Delta\rho R^3}{u^2}\right)^{0.25}$$

Implementation in COMSOL®:

$$hm = \left(\frac{D_{v,air}}{Radius}\right) \cdot 0.54 \cdot \frac{gp_{air}\Delta\rho R^3}{u^2} \left(\frac{u}{p_{air} D_{v,air}} \bullet \frac{gp_{air}(Cwpol \bullet MWwater + 1120 - p_{air}))Radius^3}{u^2}\right)^{0.25}$$

$$C_{bulk} = \frac{PP_W}{Ru \bullet Tabs}$$

8.4 Appendix D (Sensitivity Analysis of Other Parameters)

Concentration Profiles when changing the diffusivity of the barrier layer, partition coefficient between the hydrocolloid and barrier layer, mass transfer coefficient at air interface, relative humidity, thicknesses of the hydrocolloid and barrier layer.

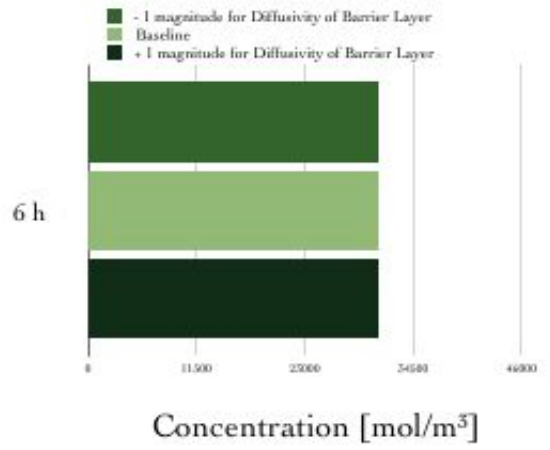

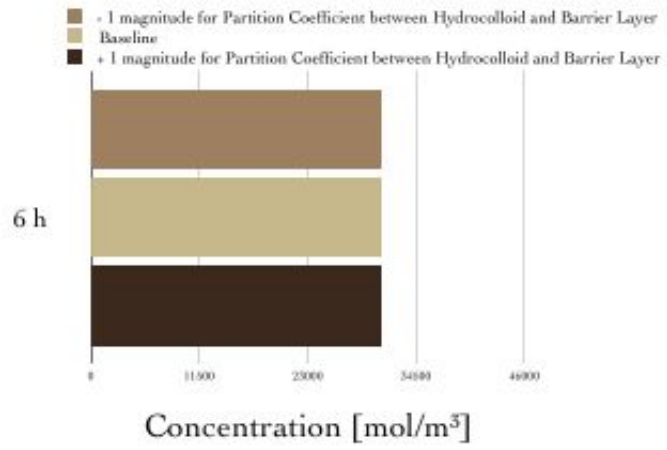

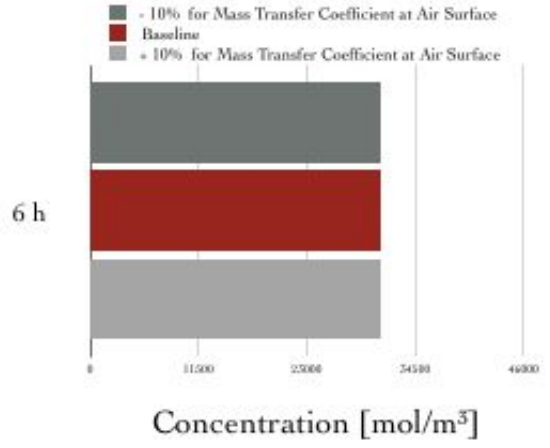

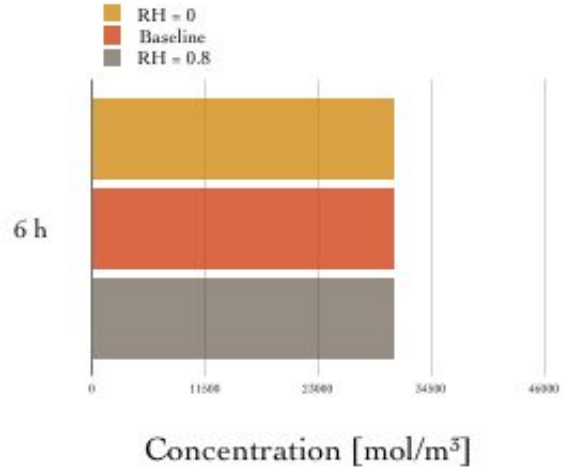

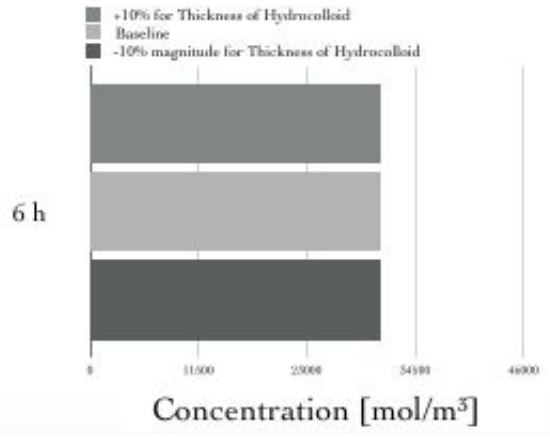

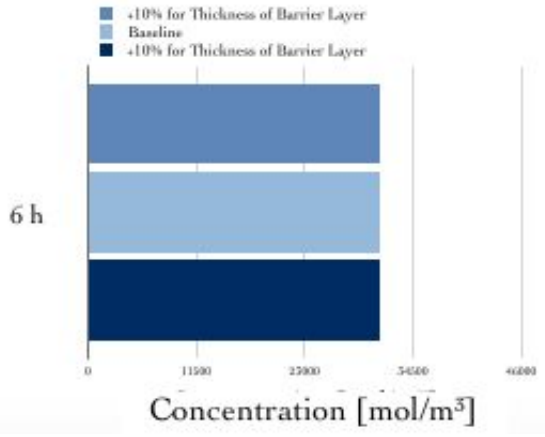

Flux Profiles when changing the diffusivity of the barrier layer, partition coefficient between the hydrocolloid and barrier layer, mass transfer coefficient at air interface, relative humidity, thicknesses of the hydrocolloid and barrier layer.

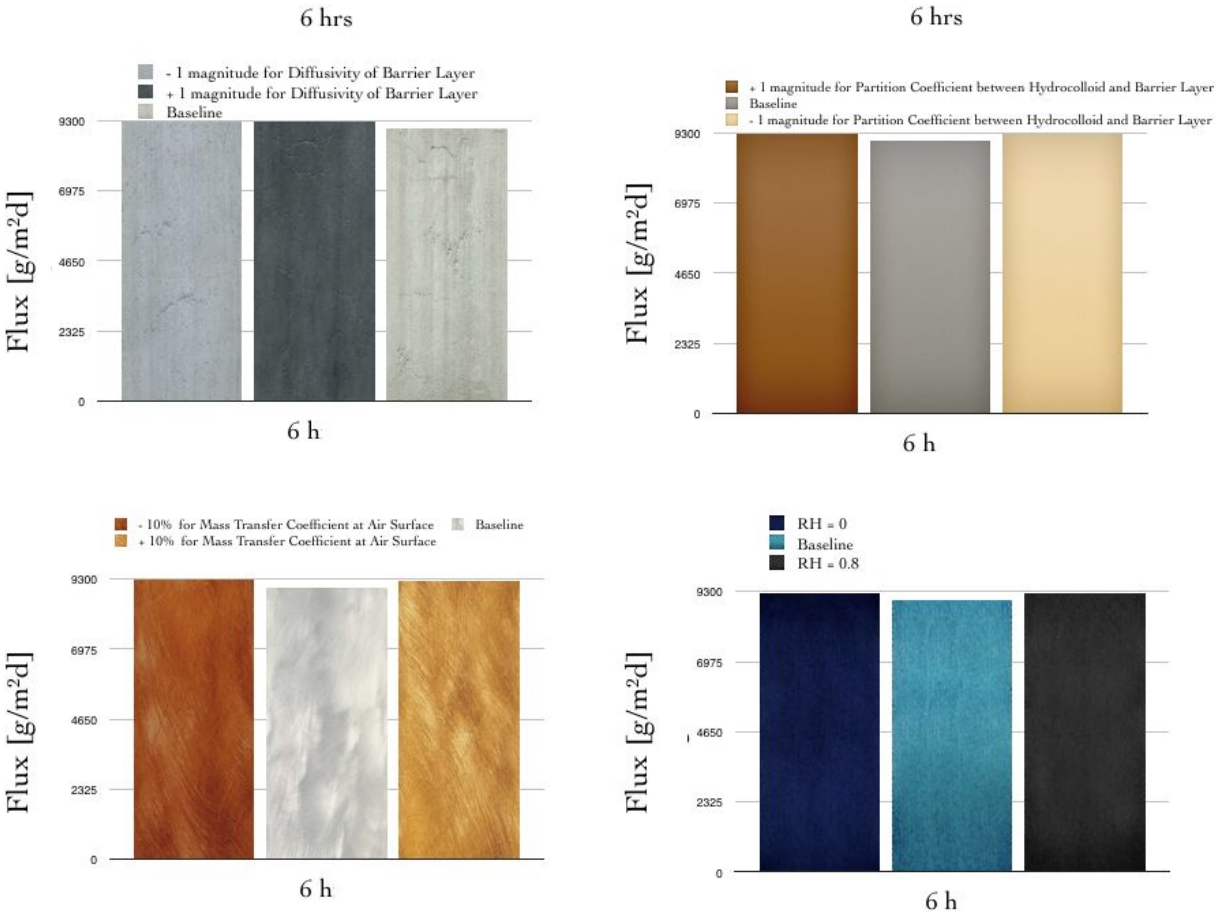

9.0 References

[1] Xu, Rui, et al. “Controlled Water Vapor Transmission Rate Promotes Wound-Healing via Wound Re-Epithelialization and Contraction Enhancement.” Scientific Reports, vol. 6, no. 1, 2016, doi:10.1038/srep24596.

[2] Bolton, Laura & Monte, K & Pirone, LA. (2000). Moisture and healing: Beyond the jargon. Ostomy/wound management. 46. 51S-62S; quiz 63S.

[3] Winter, George D. “Formation of the Scab and the Rate of Epithelization of Superficial Wounds in the Skin of the Young Domestic Pig.” Nature, vol. 193, no. 4812, 1962, pp. 293–294., doi:10.1038/193293a0.

[4] Scheuplein, R. J., and I. H. Blank. “Permeability of the Skin.” Physiological Reviews, vol. 51, no. 4, 1971, pp. 702–747., doi:10.1152/physrev.1971.51.4.702.

[5] Kamoun, Elbadawy A., et al. “A Review on Polymeric Hydrogel Membranes for Wound Dressing Applications: PVA-Based Hydrogel Dressings.” Journal of Advanced Research, vol. 8, no. 3, 2017, pp. 217–233., doi:10.1016/j.jare.2017.01.005.

[6] Wu, P., and J.d.s. Gaylor. “A Model of Water Vapour Transmission in Hydrocolloid Wound Dressings.” Journal of Membrane Science, vol. 97, 1994, pp. 27–36., doi:10.1016/0376-7388(94)00145-o.

[7] Pirone, L A, et al. “Wound Healing under Occlusion and Non-Occlusion in Partial-Thickness and Full-Thickness Wounds in Swine.” WOUNDS: A Compendium of Clinical Research and Practice, vol. 2, no. 2, 1990, pp. 74–81.

[8] Nakagawa, Noriaki, et al. “In Vivo measurement of the Water Content in the Dermis by Confocal Raman Spectroscopy.” Skin Research and Technology, vol. 16, no. 2, 2010, pp. 137–141., doi:10.1111/j.1600-0846.2009.00410.x.

[9] Flory, Paul J., and John Rehner. “Statistical Mechanics of Cross‐Linked Polymer Networks I. Rubberlike Elasticity.” The Journal of Chemical Physics, vol. 11, no. 11, 1943, pp. 512–520., doi:10.1063/1.1723791.

[10] Porter, Timothy, et al. “Models of Hydrogel Swelling with Applications to Hydration Sensing.” Sensors, vol. 7, no. 9, 2007, pp. 1980–1991., doi:10.3390/s7091980.

[11] Christensen, Christian U. “Effect of Arterial Perfusion on Net Water Flux and Active Sodium Transport across the Isolated Skin Of Bufo Bufo Bufo (L.).” Journal of Comparative Physiology ? B, vol. 93, no. 2, 1974, pp. 93–104., doi:10.1007/bf00696264.

[12] Kemanade, van, P M. “Water and Ion Transport through Intact and Damaged Skin.” Technische Universiteit Eindhoven, 15 June 1998. doi: 10.6100/IR512011.

[13] Datta, A.K. and V. Rakesh. 2010. "An Introduction to Modeling of Transport Processes: Applications to Biomedical Systems." Cambridge University Press.

[14] Blank, Irvin H., et al. "The Diffusion of Water Across the Stratum Corneum As a Function of Its Water Content." Journal of Investigative Dermatology, vol. 82, no. 2, 1984, pp. 188–194., doi:10.1111/1523-1747.ep12259835.

[15] Scholander, P. F., et al. "Negative Pressure in the Interstitial Fluid of Animals." Science, vol. 161, no. 3839, 1968, pp. 321–328., doi:10.1126/science.161.3839.321.

[16] Bishop, S.m., et al. "Importance of Moisture Balance at the Wound-Dressing Interface." Journal of Wound Care, vol. 12, no. 4, 2003, pp. 125–128., doi:10.12968/jowc.2003.12.4.26484.

[17] Michel, Cc. "Starling: the Formulation of His Hypothesis of Microvascular Fluid Exchange and Its Significance after 100 Years." Experimental Physiology, vol. 82, no. 1, Jan. 1997, pp. 1–30., doi:10.1113/expphysiol.1997.sp004000.

[18] Lohmann, Nadine, et al. "Glycosaminoglycan-Based Hydrogels Capture Inflammatory Chemokines and Rescue Defective Wound Healing in Mice." Science Translational Medicine, vol. 9, no. 386, 2017, doi:10.1126/scitranslmed.aai9044.

[19] Jones, Vanessa, et al. "Wound Dressings." Bmj, vol. 332, no. 7544, 2006, pp. 777–780., doi:10.1136/bmj.332.7544.777.

[20] Sekkat, N., et al. "Biophysical Study of Porcine Ear Skin In Vitro and Its Comparison to Human Skin In Vivo." Journal of Pharmaceutical Sciences, vol. 91, no. 11, 2002, pp. 2376–2381., doi:10.1002/jps.10220.

[21] Lamke, Lars-Olof. "Evaporative Water Loss from Burns Under Different Environmental Conditions." Scandinavian Journal of Plastic and Reconstructive Surgery, vol. 5, no. 2, 1971, pp. 77–81., doi:10.3109/02844317109042942.

[22] Picard, A, et al. "Revised Formula for the Density of Moist Air (CIPM-2007)." Metrologia, vol. 45, no. 2, 2008, pp. 149–155., doi:10.1088/0026-1394/45/2/004.

[23] *NASA*, NASA, www.grc.nasa.gov/www/BGH/viscosity.html.

[24] Galey, William R, et al. "The In Vitro Permeability Of Skin And Buccal Mucosa To Selected Drugs And Tritiated Water." Journal of Investigative Dermatology, vol. 67, no. 6, 1976, pp. 713–717., doi:10.1111/1523-1747.ep12598596.

[25] Mackie, Bruce S. "DRY EPIDERMAL DENSITY. A Study in Normal and Atopic Subjects." British Journal of Dermatology, vol. 79, no. 7, 1967, pp. 411–415., doi:10.1111/j.1365-2133.1967.tb11521.x.

[26] CROW. "Polymer Properties Database." Acetate Fibers, polymerdatabase.com/polymer physics/Polymer Density.html.

[27] Kalia, Yogeshvar N., et al. “Normalization of Stratum Corneum Barrier Function and Transepidermal Water Loss In Vivo.” SpringerLink, Springer, Dordrecht, link.springer.com/content/pdf/10.1023/A:1026474200575.

[28] “American Meteorological Society.” An Assessment of the Primary Sources of Spread of Global Warming Estimates from Coupled Atmosphere–Ocean Models: Journal of Climate: Vol 21, No 19, journals.ametsoc.org/doi/citedby/10.1175/1520-0469(1947)004<0193:VATCOA>2.0.CO;2.

[29] Frei, Walter. “Model Translational Motion with the Deformed Mesh Interfaces.” *COMSOL* , www.comsol.com/blogs/model-translational-motion-with-the-deformed-mesh-interfaces/.

Team member name	Jackson Cabot	Robert Klein	Grainger Sasso	Viola Zhang	NOT DONE
Wrote abstract		X	X	X	
Edited abstract		X	X	X	
Wrote introduction			X	X	
Edited introduction		X	X	X	
Wrote method section		X	X	X	
Edited method section		X	X	X	
Wrote results section		X	X	X	
Edited results section		X	X	X	
Wrote discussion section		X			
Edited discussion section		X	X	X	
Wrote summary and conclusion section		X			
Edited summary and conclusion section		X	X	X	
Wrote bibliography section		X			
Edited bibliography section		X	X	X	
Prepared processed data table for appendix		X	X	X	
Checked data in processed data table in appendix		X	X	X	
Prepared figures or tables for main text		X	X	X	
Checked figures or tables in main text		X	X	X	
Assigned tasks to group members		X	X	X	
Put the report together from the parts provided by others		X	X	X	
Read and edited entire document to check for consistency		X	X	X	